ISSP-CMSI International Workshop/Symposium on
Material Simulation in Petaflops era (MASP2012)
June 27, 2012
ISSP, Univ. Tokyo

Real-time electron dynamics in solids under strong electromagnetic fields

Kazuhiro Yabana
Center for Computational Sciences, University of Tsukuba

Y. Shinohara	U. Tsukuba
S.A. Sato	U. Tsukuba
T. Sugiyama	U. Tsukuba
T. Otobe	JAEA
J.-I. Iwata	U. Tokyo
G.F. Bertsch	U. Washington

TDDFT: First-principles tool for electron dynamics simulation

$$i\hbar \frac{\partial}{\partial t}\psi_i(\vec{r},t) = \{h_{KS}[\rho(\vec{r},t)] + V_{ext}(\vec{r},t)\}\psi_i(\vec{r},t)$$

$$\rho(\vec{r},t) = \sum_i |\psi_i(\vec{r},t)|^2$$

Linear response regime
(Perturbation theory)

Electronic excitation

Absorption cross section

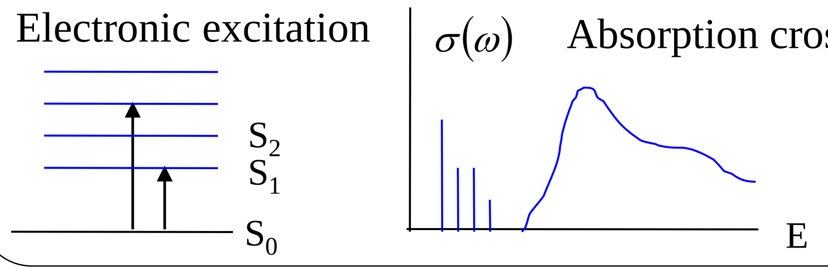

Laser-solid interaction

Dielectric function

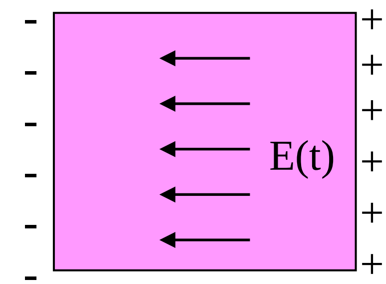

Coherent phonon
Electron-hole plasma
Optical breakdown

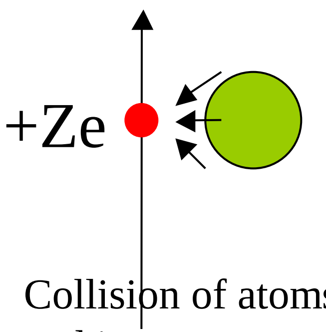

Collision of atoms and ions

Intense, ultra-short Laser pulses

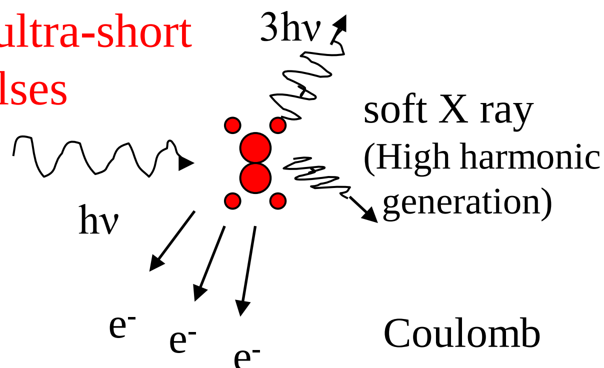

Coulomb explosion

Multiple ionization

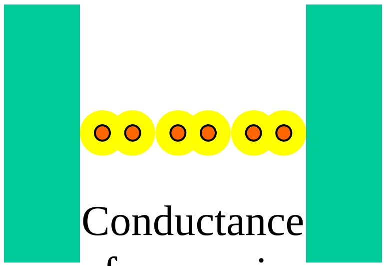

Conductance of nano-wire

Nonlinear, nonperturbative regime
(Initial value problem)

CONTENTS

1. A frontier in light - matter interaction : intense and ultrashort

   - Theories and computations required in current optical sciences -

2. Real-time and real-space calculation for electron dynamics in solid

   - time-dependent band calculation, treatment of boundaries. -

3. Electron and phonon dynamics in solid for a given electric field

   - Dielectric function, coherent optical phonon, optical breakdown, … -

4. Coupled Maxwell + TDDFT multiscale simulation

   - First-principles simulation for macroscopic electromagnetic field in intense regime, Dense electron-hole plasma induced by intense laser pulses -

Modern experiments on light-matter interactions

Requiring new theories and large-scale computations,
beyond ordinary electromagnetism and quantum mechanics

- Nano-sized material
  too large to calculate microscopically, too small to calculate macroscopically.
  $\longrightarrow$ large-scale microscopic calculation

- Near field optics (resolution beyond diffraction limit)
- Meta-material (negative refractive index)
- Surface plasmon polariton (coupled light-electron dynamics)
  $\longrightarrow$ quantum effects (?)

- Intense and ultrashort laser pulses (extreme nonlinear electron dynamics)
  $\longrightarrow$ requiring time-domain description,
  coupled dynamics of electrons and electromagnetic fields

Frontiers in Optical Sciences: Intense field

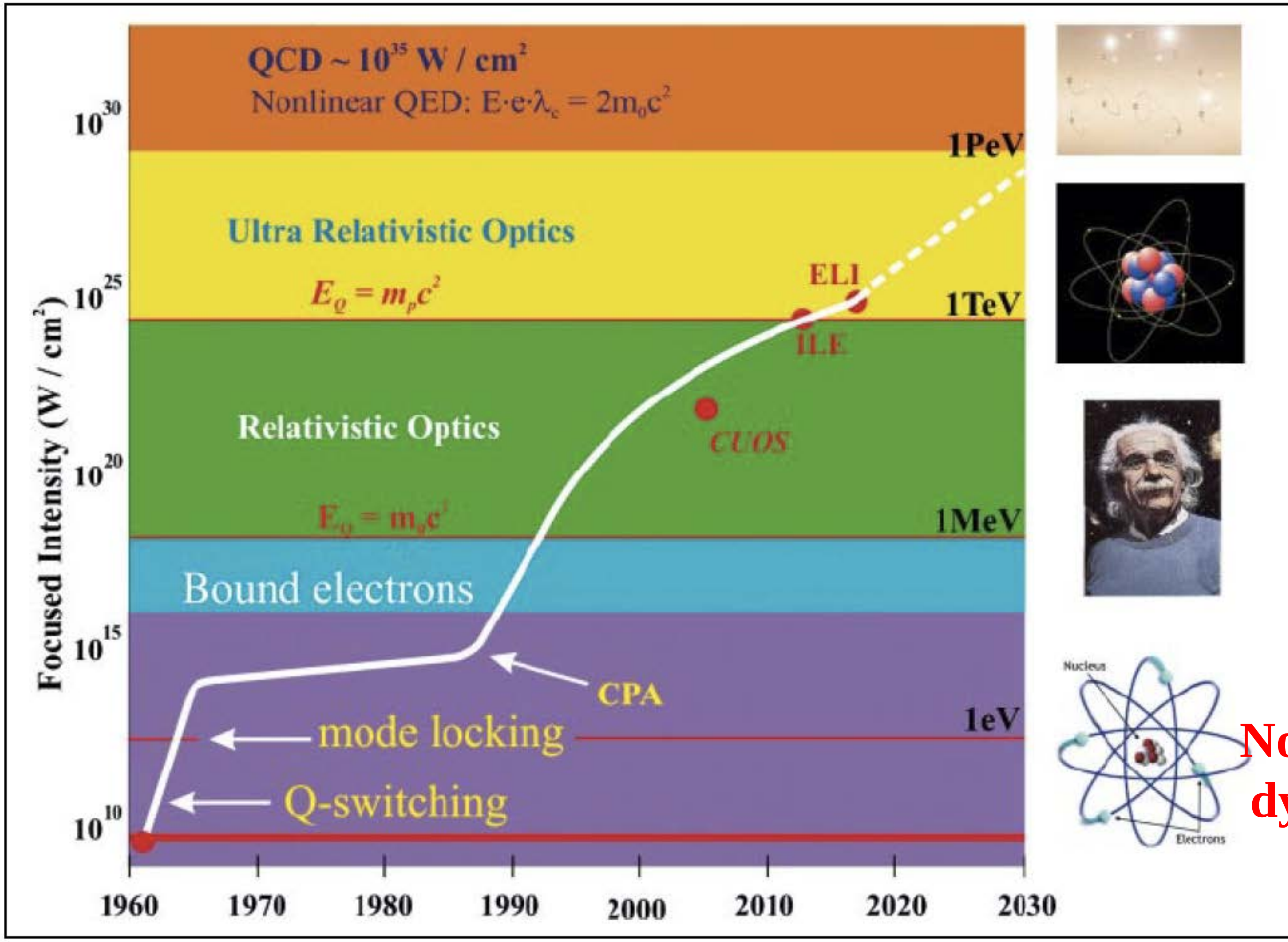

FIG. 1: **Maximum laser intensity as a function of time and fields of research accessible with these intensities.**

QED Vacuum breakdown

Nuclear reaction, Particle Acceleration

Relativistic Classical

Nonlinear electron dynamics

Nonrelativistic Quantum

G. Mourou Optik & Photonik December 2010 No. 4

Intense laser pulse on solid

Laser intensity

$10^{13} - 10^{15}\,\mathrm{W/cm^2}$

Nonlinear optics

Coherent phonon

HHG

Electron-hole plasma
Optical breakdown
Laser machining

Laser acceleration

Vacuum breakdown

Nonrelativistic
Quamtum mechanics

Relativistic
Classical mechanics

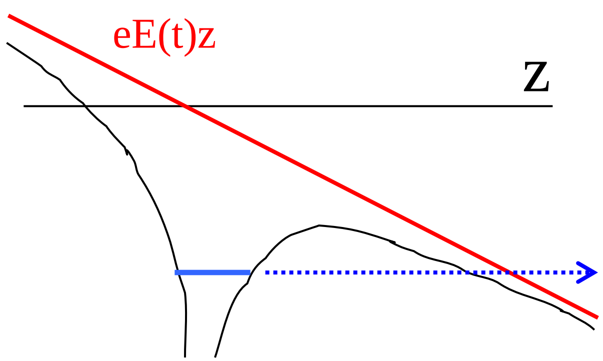

External electric field by laser pulse

≈ Internal electric field by nuclei

Frontiers in Optical Sciences: Ultra-short dynamics

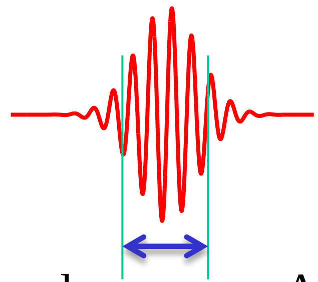

Picosecond 10^{-12}s

Femtosecond 10^{-15}s

Attosecond 10^{-18}s

10^{-23}s

Time

Period of Optical phonon (Si, 64 fs)

Period of electron orbital in Hydrogen, 150as

Period of Ti-sapphire laser pulse

Shortest laser pulse 80 as (2008)

Nucleon motion in nucleus

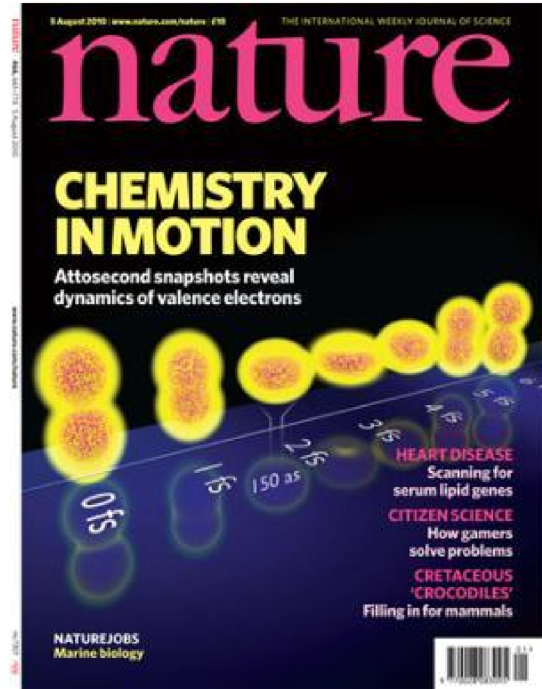

Real-time observation of valence electron motion
E. Goulielmakis et.al, Nature 466, 739 (2010).

Pump-Probe Measurement: Coherent Phonon

Intense 1st pulse excites electrons and atoms.
Weak 2nd pulse measure change of reflectivity.

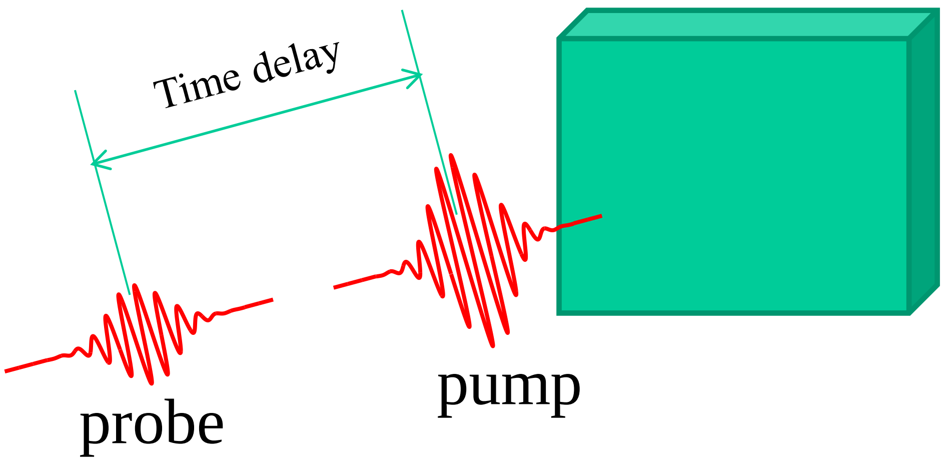

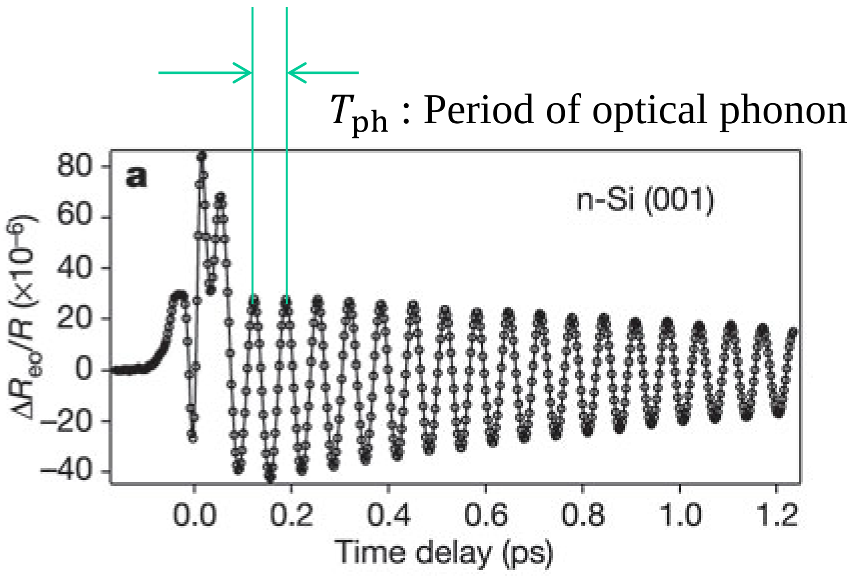

M. Hase, et al. Nature (London) 426, 51 (2003)

$$\frac{\Delta R(t)}{R} \propto e^{-\Gamma t} \sin(\Omega_{\mathrm{ph}} t + \phi)$$

Femto-technology: nonthermal machining by femtosecond laser pulses

Figure B1 Femtosecond laser micromaching process. **a**, Schematic of the laser incident on a transparent material. **b**, Diagram of the excitation of electrons to the conduction band. **c**, Microscope images showing the large variation in the feature characteristics depending on the experimental conditions. Left: single 10-nJ pulse and right: 25,000 5-nJ pulses at a frequency of 25 MHz (both with the same focal spot).

R.R. Gattass, E. Mazur, Nature Photonics 2, 220 (2008).

Micromachining – waveguide-

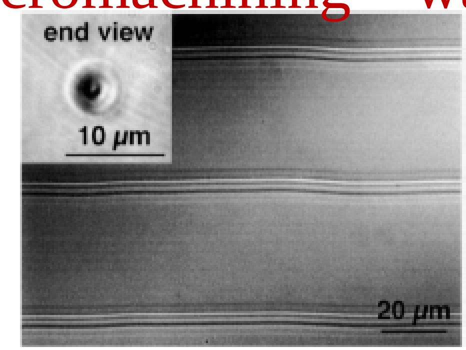

Optical microscope image of waveguides written inside bulk glass by a 25-MHz train of 5-nJ sub-100-fs pulses, C.B. Schaffer et.al, OPTICS LETTERS 26, 93 (2001)

Nanosurgery

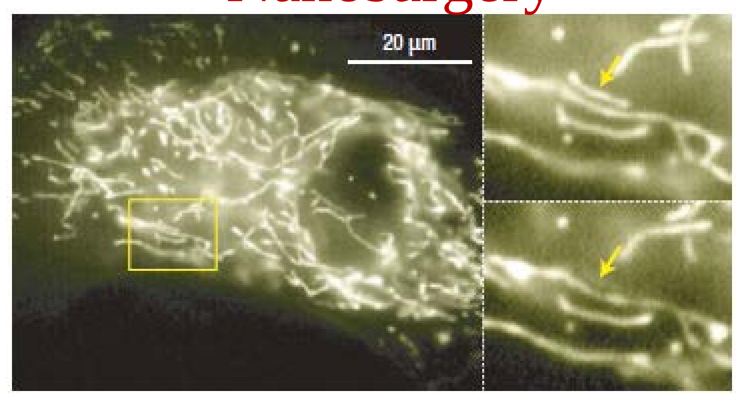

Ablation of a single mitochondrion in a living cell.
N. Shen et.al, Mech. Chem. Biosystems, 2, 17 (2005).

CONTENTS

1. A frontier in light - matter interaction : intense and ultrashort

   - Theories and computations required in current optical sciences -

2. Real-time and real-space calculation for electron dynamics in solid

   - time-dependent band calculation, treatment of boundaries. -

3. Electron and phonon dynamics in solid for a given electric field

   - Dielectric function, coherent optical phonon, optical breakdown, … -

4. Coupled Maxwell + TDDFT multiscale simulation

   - First-principles simulation for macroscopic electromagnetic field in intense regime,
   Dense electron-hole plasma induced by intense laser pulses -

Calculation in real-time and real-space

Time-dependent Kohn-Sham equation

$$i\hbar \frac{\partial}{\partial t}\psi_i(\vec{r},t) = h_{KS}[n(\vec{r},t)]\psi_i(\vec{r},t) \qquad n(\vec{r},t) = \sum_i |\psi_i(\vec{r},t)|^2$$

$$h_{KS}[n(\vec{r},t)] = -\frac{\hbar^2}{2m}\nabla^2 + \underline{V_{ion}(\vec{r})} + \int d\vec{r}\,' \frac{e^2}{|\vec{r}-\vec{r}\,'|} + \mu_{xc}[n(\vec{r},t)] + V_{ext}(\vec{r},t)$$

Norm-conserving pseudopotential

3D real-space grid representation, high order finite difference

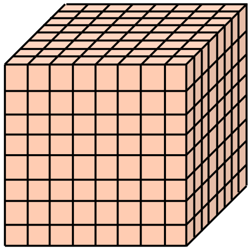

$$-\frac{\hbar^2}{2m}\left[\sum_{n_1=-N}^{N} C_{n_1}\psi(x_i+n_1h, y_j, z_k) + \sum_{n_2=-N}^{N} C_{n_2}\psi(x_i, y_j+n_2h, z_k) + \sum_{n_3=-N}^{N} C_{n_3}\psi(x_i, y_j, z_k+n_3h)\right]$$
$$+[V_{\rm ion}(x_i,y_j,z_k)+V_H(x_i,y_j,z_k)+V_{\rm xc}(x_i,y_j,z_k)]\psi(x_i,y_j,z_k)=E\psi(x_i,y_j,z_k)\ .$$

Time evolution: 4-th order Taylor expansion

$$\psi_i(t+\Delta t) = \exp\left[\frac{h_{KS}(t)\Delta t}{i\hbar}\right]\psi_i(t) \approx \sum_{k=0}^{N}\frac{1}{k!}\left(\frac{h_{KS}(t)\Delta t}{i\hbar}\right)\psi_i(t), \qquad N=4$$

Treatment of optical electric field

We assume a long wavelength limit, lattice const. << light wavelength

⬇

Electron dynamics in a unit cell under time-dependent, spatially uniform field

Two key issues

Use (spatially uniform) vector potential instead of (spatially linear) scalar potential to express macroscopic electric field.

Boundary effect (macroscopic shape effect) needs to be considered from outside of the theory.

Electron dynamics in crystalline solid under spatially uniform field

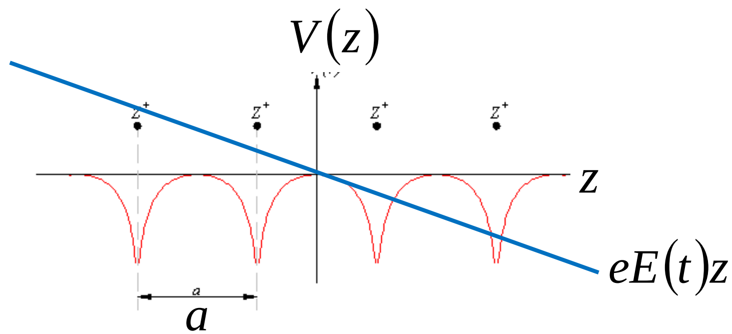

Scalar potential $eE(t)z$ spoils spatial periodicity of the Hamiltonian

$$h(\vec{r}+\vec{a}) \neq h(\vec{r})$$

Employing a vector potential replacing the scalar potential, one may recover the periodicity of the Hamiltonian

Time-dependent, spatially uniform electric field

$$\vec{E} = -\vec{\nabla}\phi - \frac{1}{c}\frac{\partial \vec{A}}{\partial t}$$

$$\phi = E(t)z \quad \Leftrightarrow \quad \underline{\vec{A}(t) = c\int^{t} dt' E(t')\hat{z}}$$

$$i\hbar\frac{\partial}{\partial t}\psi(t) = \left[\frac{1}{2m}\left(\vec{p} - \frac{e}{c}\vec{A}(t)\right)^2 + V(\vec{r},t)\right]\psi(t)$$

$$h(\vec{r}+\vec{a}) = h(\vec{r}) \qquad \underline{\psi_{nk}(\vec{r}+\vec{a}) = e^{i\vec{k}\vec{a}}\psi_{nk}(\vec{r})}$$

Time-dependent Bloch function

Equation for time-dependent Bloch function

$$i\hbar \frac{\partial}{\partial t} u_{n\vec{k}}(\vec{r},t) = \left[\frac{1}{2m} \left(\vec{p} + i\vec{k} - \frac{e}{c}\vec{A}(t) \right)^2 + V(\vec{r},t) \right] u_{n\vec{k}}(\vec{r},t)$$

$$n(\vec{r},t) = \sum_{nk} \left| u_{n\vec{k}}(\vec{r},t) \right|^2$$

$$\psi_{nk}(\vec{r},t) = e^{i\vec{k}\vec{r}} u_{nk}(\vec{r},t)$$

$$u_{nk}(\vec{r}+\vec{a},t) = u_{nk}(\vec{r},t)$$

Electron dynamics in metallic clusters by TDDFT

K. Yabana, G.F. Bertsch, Phys. Rev. B54, 4484 (1996).

Na_{147}^{+}

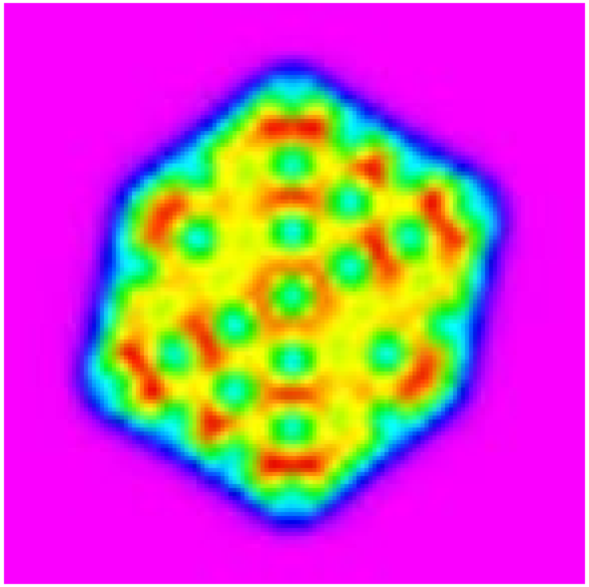

Assume
Icosahedral shape

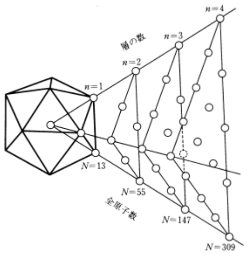

図 5・61 多層正二十面体構造(MIC)の概念図[104)]
n は MIC の層の数であり，N は全原子数である。1 層構造($n=1$)では原子数 $N=13$ に対応し，2 層構造($n=2$)では $N=55$，3 層構造($n=3$)では $N=147$…となる。

Li_{147}^{+}

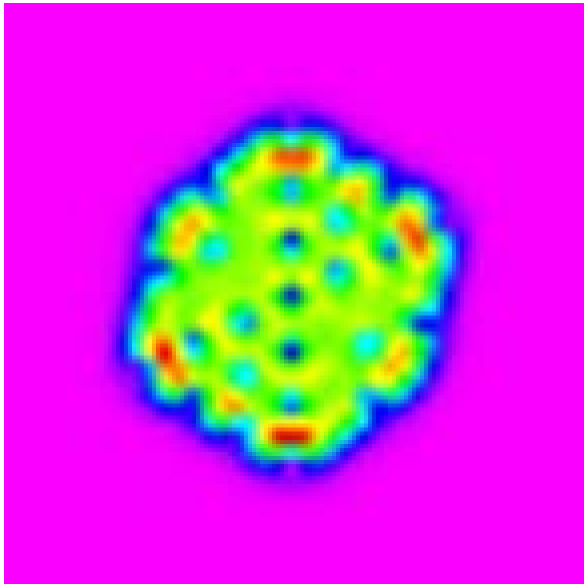

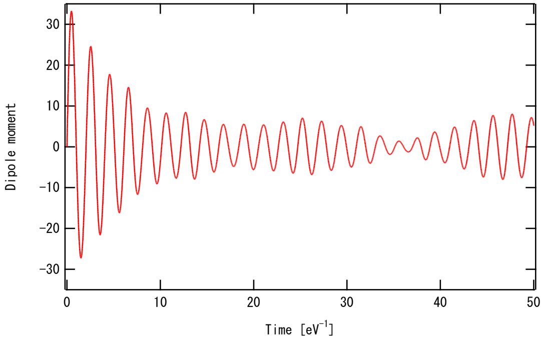

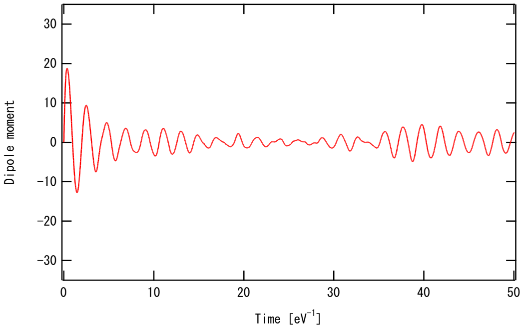

Collective electronic excitation: plasmon

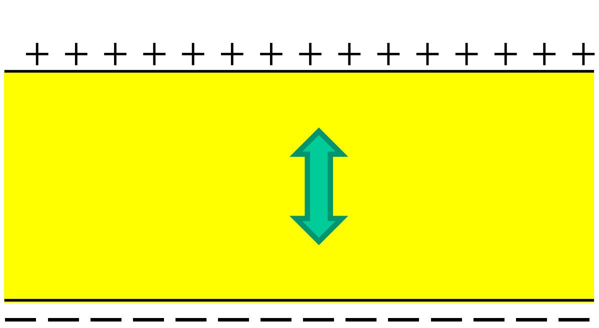

Longitudinal plasmon

$$\omega_p = \left(\frac{4\pi e^2 n}{m} \right)^{1/2}$$

n: electron density

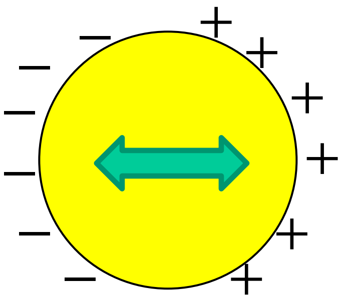

Mie plasmon
(Surface plasmon of spherical nanoparticle)

$$\omega_{Mie} = \frac{\omega_p}{\sqrt{3}}$$

Choice of geometry (boundary condition)

- We solve electron dynamics in a unit cell inside a crystalline solid.

- The electric field in the unit cell depends on macroscopic geometry of the sample.

- We need to specify the ‘boundary condition’ in the calculation.

$$i\hbar \frac{\partial}{\partial t}\psi_{nk}(t) = \left[\frac{1}{2m}\left(\vec{p} - \frac{e}{c}\vec{A}(t) \right)^2 + V(\vec{r},t) \right]\psi_{nk}(t)$$

$$\vec{E} = -\frac{1}{c}\frac{\partial \vec{A}}{\partial t} \qquad \vec{A}(t) = c\int^{t} dt' E(t')\hat{z}$$

Optical response of thin film

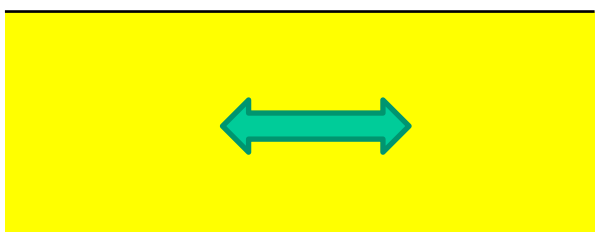

Transverse

$$A(t) = A_{ext}(t)$$

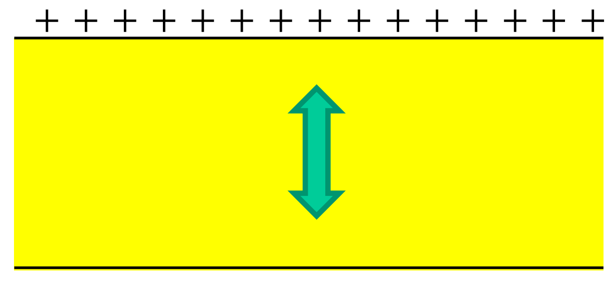

Longitudinal

$$A(t) = A_{ext}(t) + A_{polarization}(t)$$

Longitudinal geometry:
Treatment of induced polarization

Bertsch, Iwata, Rubio, Yabana, Phys. Rev. B62(2000)7998.

“parallel-plate-capacitor with dielectrics”.

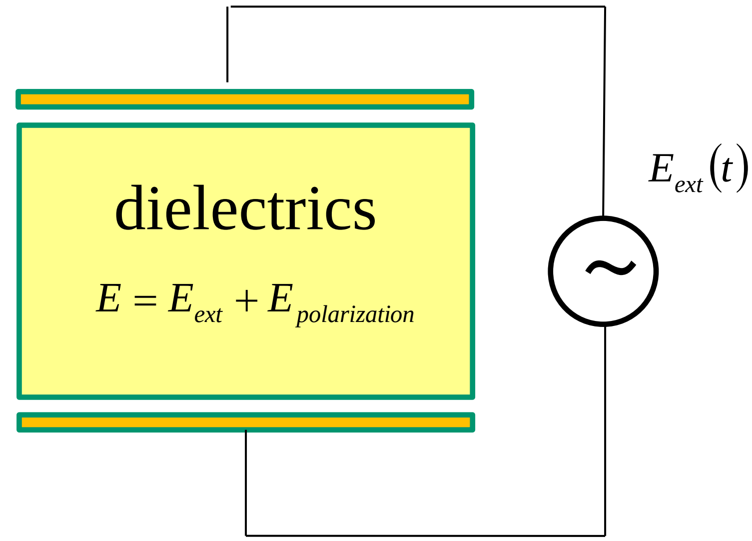

$$A(t) = A_{extr}(t) + A_{polarization}(t)$$

$$E(t) = -\frac{1}{c}\frac{\partial A(t)}{\partial t}$$

$$A(t) = -c\int^{t} E(t')dt'$$

Equation for polarization

$$\frac{d^2\vec{A}_{polarization}(t)}{dt^2} = \frac{4\pi}{\Omega}\int_{\Omega(cell)} d\vec{r}\;\vec{j}\,(\vec{r},t)$$

$\vec{A}(t)$ ↓ ↑ $\vec{j}\,(\vec{r},t)$

Time-dependent Kohn-Sham equation

$$i\hbar\frac{\partial}{\partial t}\psi_i = \frac{1}{2m}\left(-i\hbar\vec{\nabla} + \frac{e}{c}\vec{A}\right)^2\psi_i - e\phi\psi_i + \frac{\delta E_{xc}}{\delta n}\psi_i$$

$$n = \sum_i |\psi_i|^2 \qquad \vec{j} = \frac{1}{2m}\sum_i\left(\psi_i^*\left(\vec{p} + \frac{e}{c}\vec{A}\right)\psi_i - c.c.\right)$$

CONTENTS

1. A frontier in light - matter interaction : intense and ultrashort

   - Theories and computations required in current optical sciences -

2. Real-time and real-space calculation for electron dynamics in solid

   - time-dependent band calculation, treatment of boundaries. -

3. Electron and phonon dynamics in solid for a given electric field

   - Dielectric function, coherent optical phonon, optical breakdown, … -

4. Coupled Maxwell + TDDFT multiscale simulation

   - First-principles simulation for macroscopic electromagnetic field in intense regime,
   Dense electron-hole plasma induced by intense laser pulses -

Linear response:

Two methods to calculate dielectric function from real-time electron dynamics

Transverse geometry

$$J(t) = \int^{t} dt' \sigma(t-t') \left(-\frac{1}{c} \frac{dA}{dt} \right)$$

$$\sigma(\omega) = \int dt e^{i\omega t} \sigma(t)$$

$$\varepsilon(\omega) = 1 + \frac{4\pi i \sigma(\omega)}{\omega}$$

Longitudinal geometry

$$A_{tot}(t) = A_{ext}(t) + A_{pol}(t)$$

$$\frac{d^2 A_{pol}(t)}{dt^2} = 4\pi J(t)$$

$$A_{tot}(t) = \int^{t} dt' \varepsilon^{-1}(t-t') A_{ext}(t')$$

$$\frac{1}{\varepsilon(\omega)} = \frac{\int dt\, e^{i\omega t} A_{tot}(t)}{\int dt\, e^{i\omega t} A_{ext}(t)}$$

For an impulsive external field,

$$E(t) = k\delta(t), \quad A(t) = -kc\theta(t)$$

$$J(t) = k\sigma(t)$$

$$E_{tot}(t) = -\frac{1}{c} \frac{dA_{tot}}{dt} = k\varepsilon^{-1}(t)$$

Comparison of numerical results for dielectric function of Si by two methods

- Green : longitudinal
- Red : transverse

Spatial grid: 16^3
K-points : 8^3

Distortion strength:
A_0 = 0.01 (with induced),
0.0005 (without)

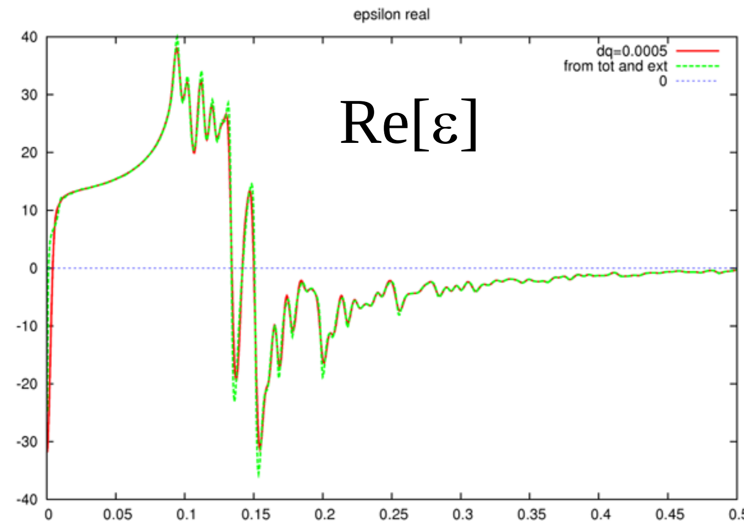

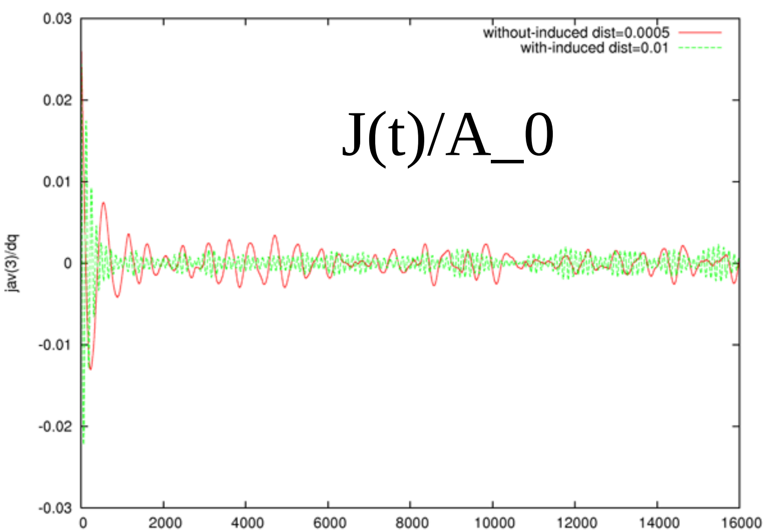

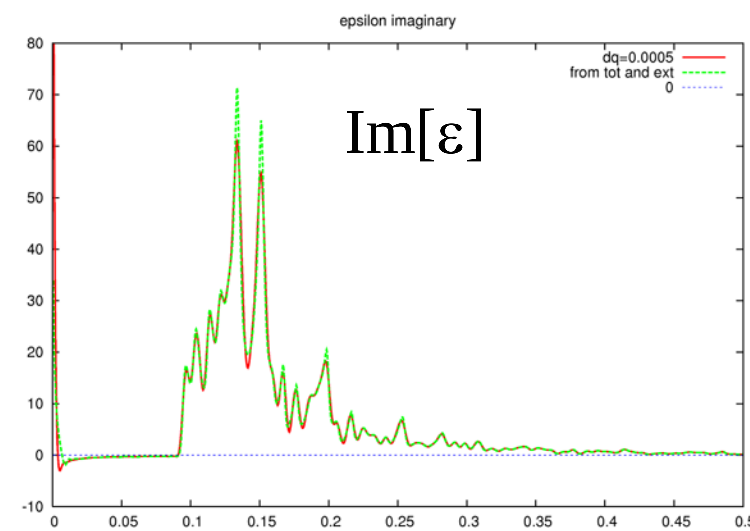

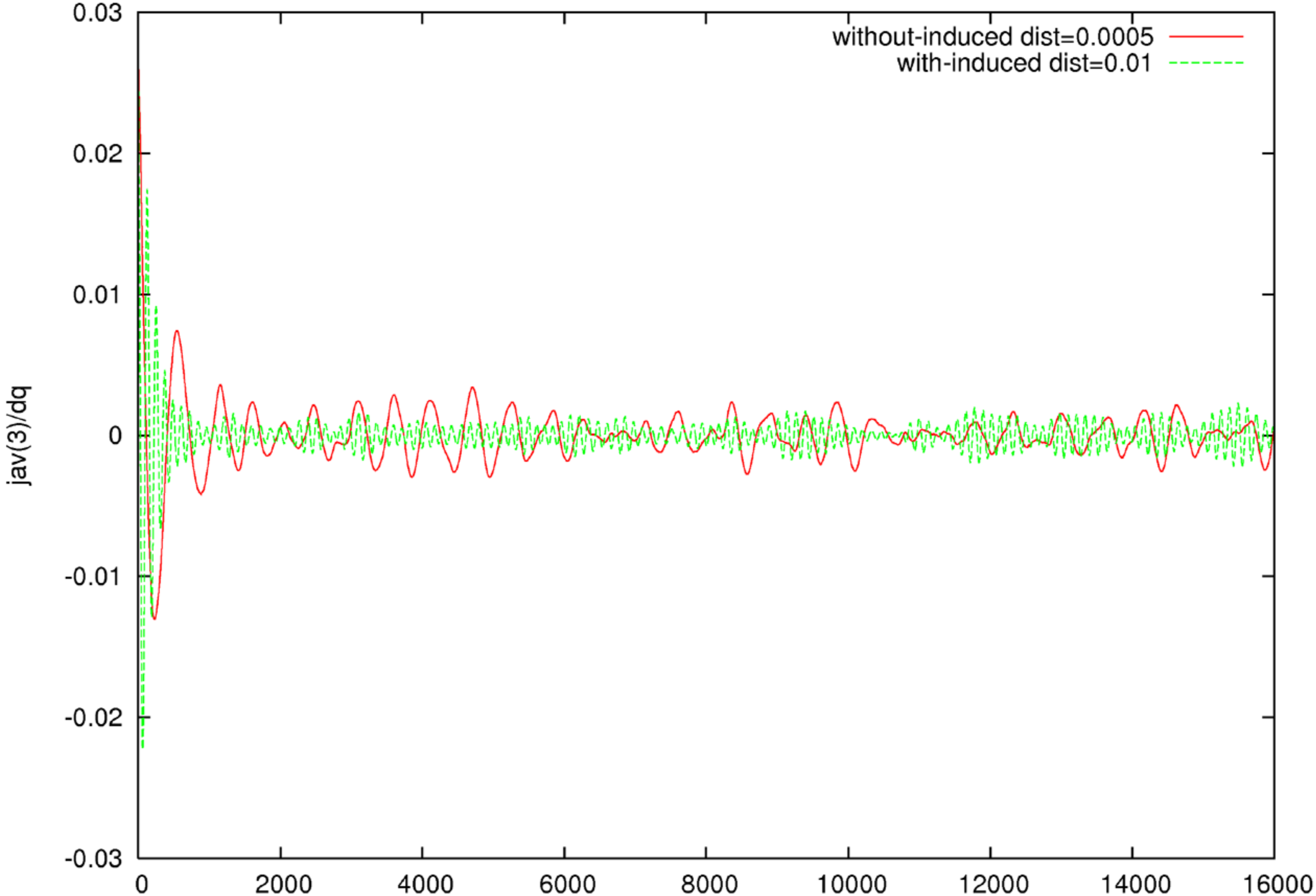

0.03
0.02
0.01
0
-0.01
-0.02
-0.03
0
2000
4000
6000
8000
10000
12000
14000
16000
jav(3)/dq
without-induced dist=0.0005
with-induced dist=0.01

Dielectric function of Si in TDDFT (ALDA)

Transverse calculation

Instantaneous pulse field is applied at t=0,
the induced current as a function of time.

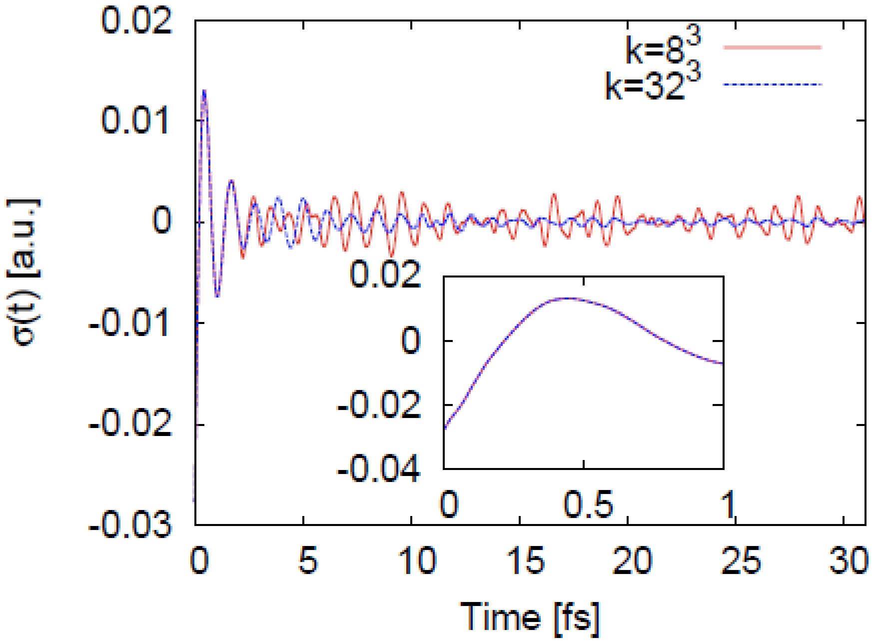

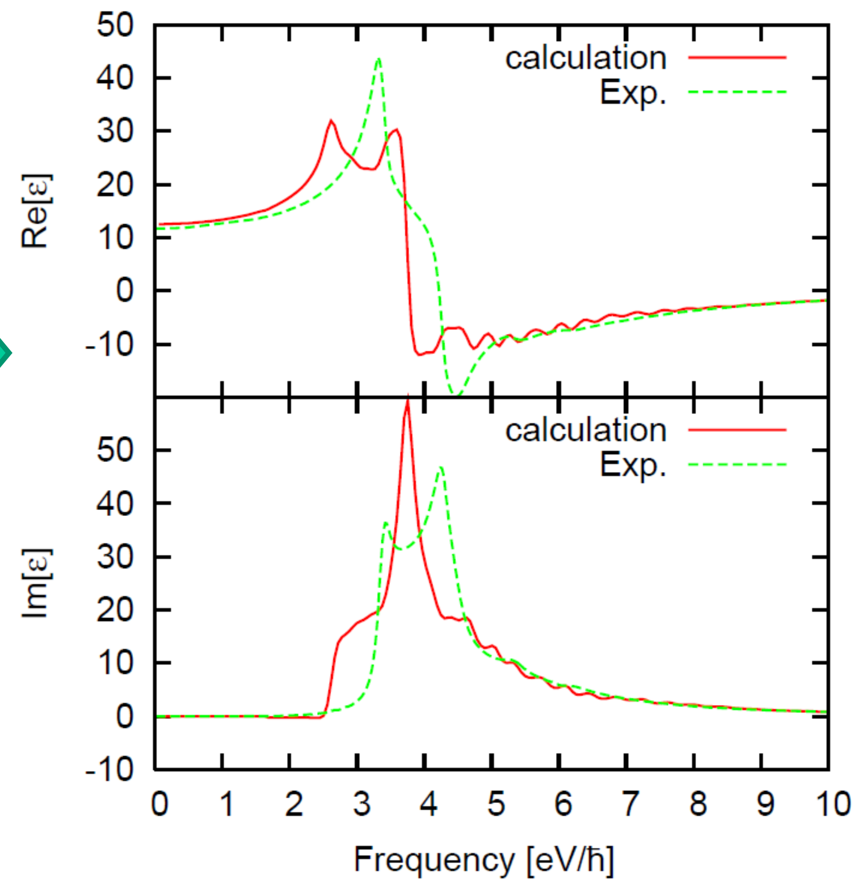

Dielectric function by TDDFT (ALDA) is not very good.
Too small bandgap (common problem with LDA).

Dots: experiment
Dash-dotted: RPA
Solid: Bethe-Salpeter
(electron-hole interaction considered)

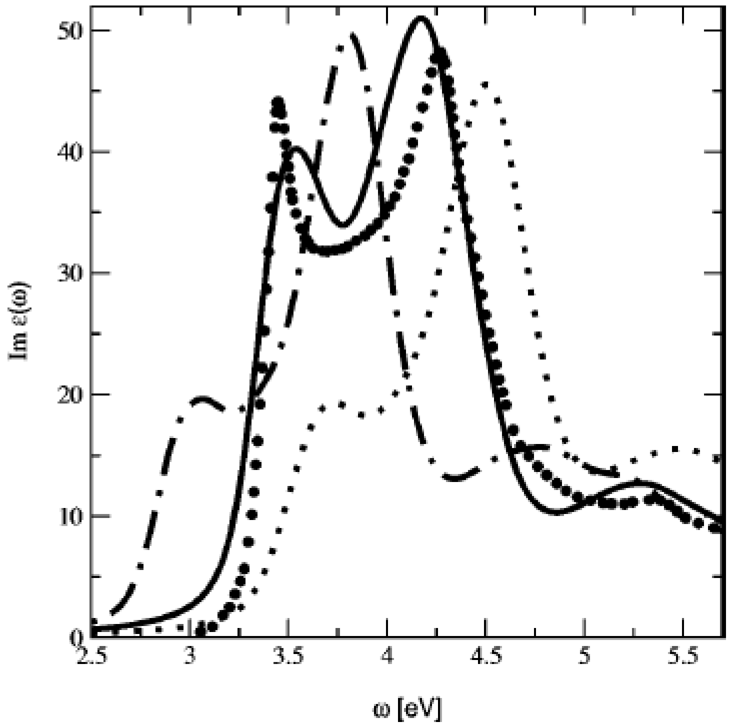

FIG. 5. Silicon absorption spectrum [Im(ε_M)]: ●, experiment (Lautenschlager *et al.*, 1987); dash-dotted curve, RPA, including local field effects; dotted curve, *GW*-RPA; solid curve, Bethe-Salpeter equation.

G. Onida, L. Reining, A. Rubio,
Rev. Mod. Phys. 74(2002)601.

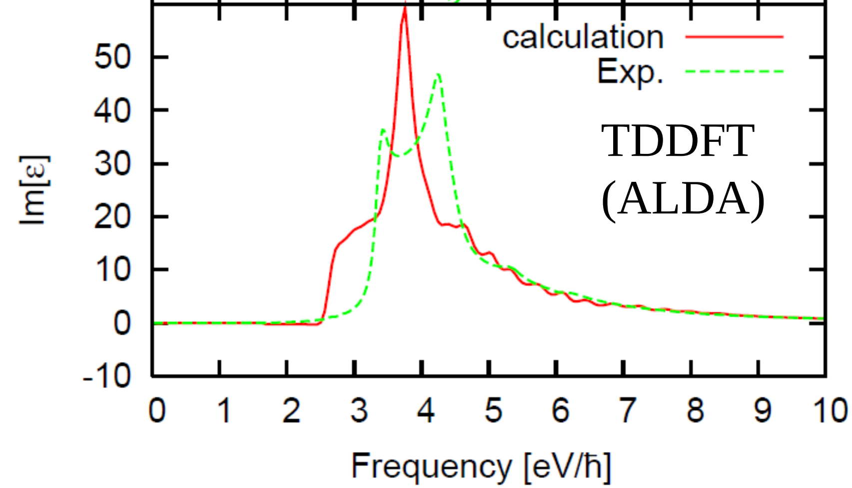

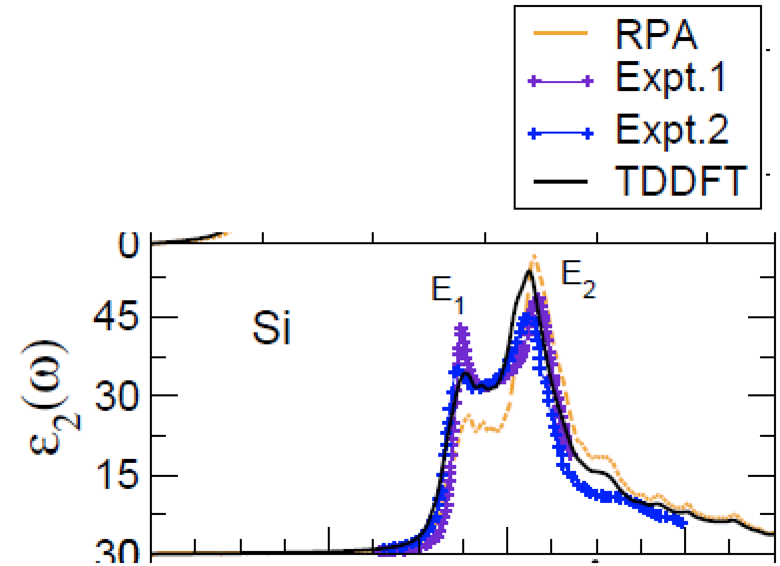

PRL107, 186401 (2011) , arXiv:1107.0199
S. Sharma, J.K. Dewhurst, A. Sanna, E.K.U. Gross,
Bootstrap approx. for the exchange-correlation kernel of time-dependent density functional theory

Pump-Probe Measurement: Coherent Phonon

Intense 1st pulse excites electrons and atoms.
Weak 2nd pulse measure change of reflectivity.

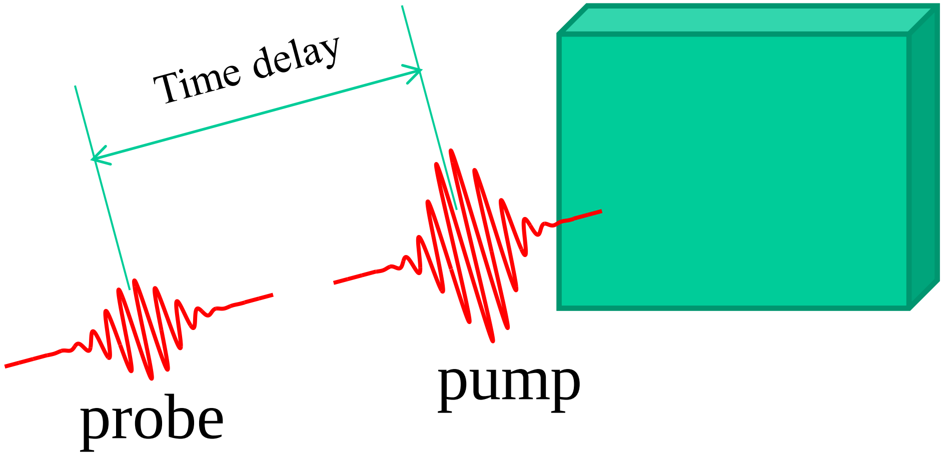

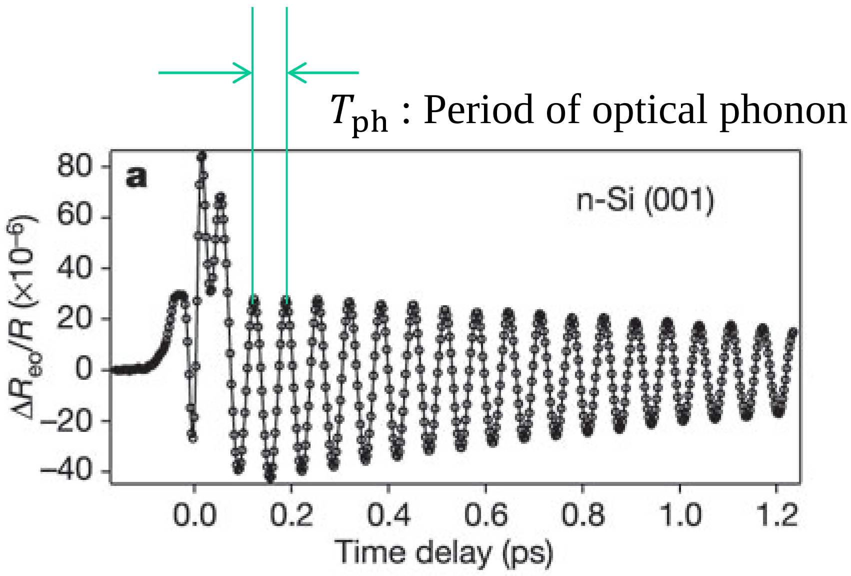

M. Hase, et al. Nature (London) 426, 51 (2003)

$$\frac{\Delta R(t)}{R} \propto e^{-\Gamma t} \sin\left(\Omega_{\mathrm{ph}} t + \phi\right)$$

The two mechanisms for coherent phonon generation

Virtual electronic excitation (transparent material)

Real electronic excitation (opaque material)

$$V = \frac{1}{2}\chi|E(t)|^2, \quad F = -\frac{\partial V}{\partial q}$$

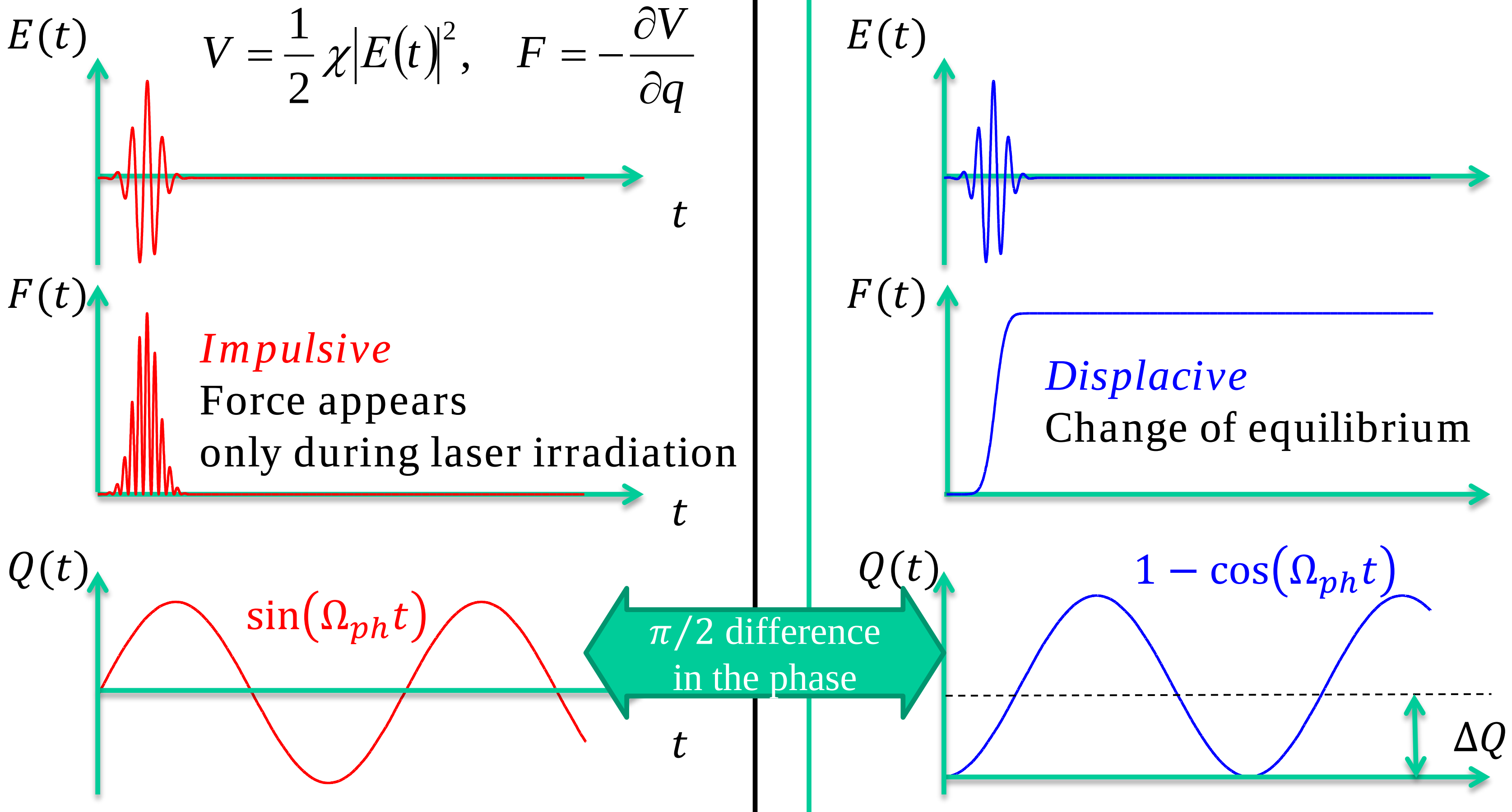

Y. Yan, E. Gamble, and K. Nelson, J. Chem. Phys. **83**, 5391 (1985)

H.J. Zeiger, J. Vidal, T.K. Cheng, E.P. Ippen, G. Dresselhaus, and M.S. Dresselhaus, Phys. Rev. B **45**, 768 (1992)

Coherent phonon measurements in Sb

- Most popular material for coherent phonon generation
- Observed two modes: A_{1g}, E_g

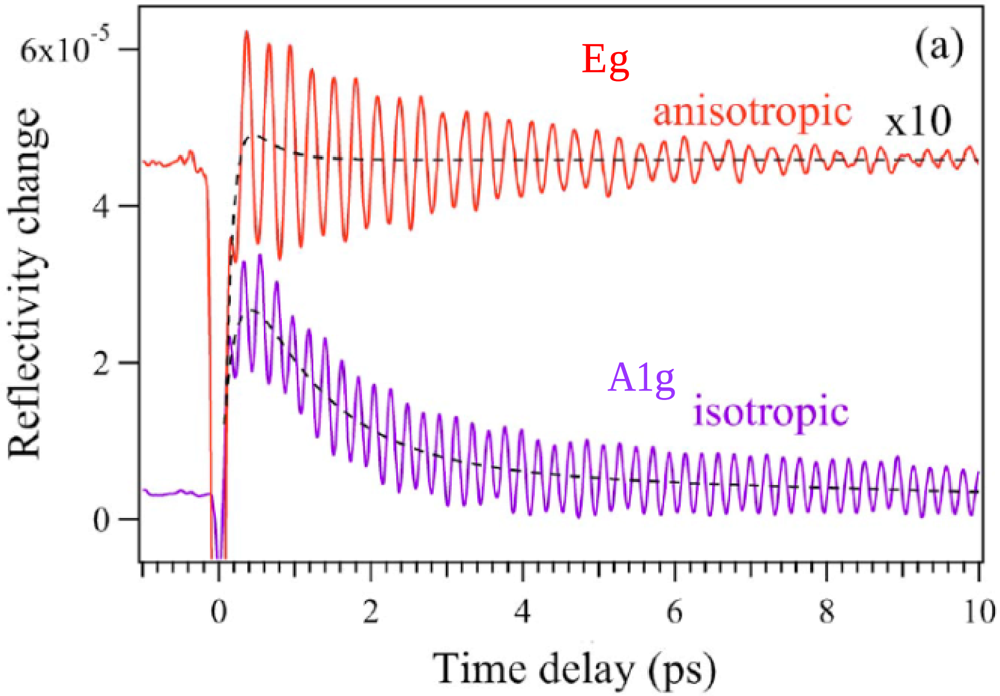

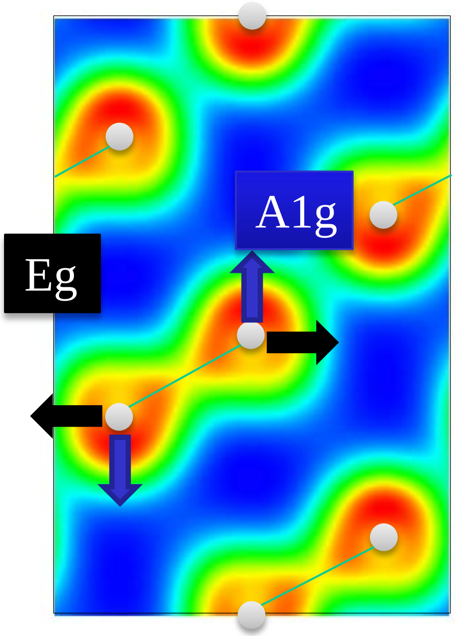

K. Ishioka, M Kitajima, and O. Misochko, J. Appl. Phys. **103**, 123505 (2008)

Sb: crystal structure and phonon mode

- Semimetal
- Rhombohedral structure

  Having C3 symmetry axis parallel to vertical line in following figure

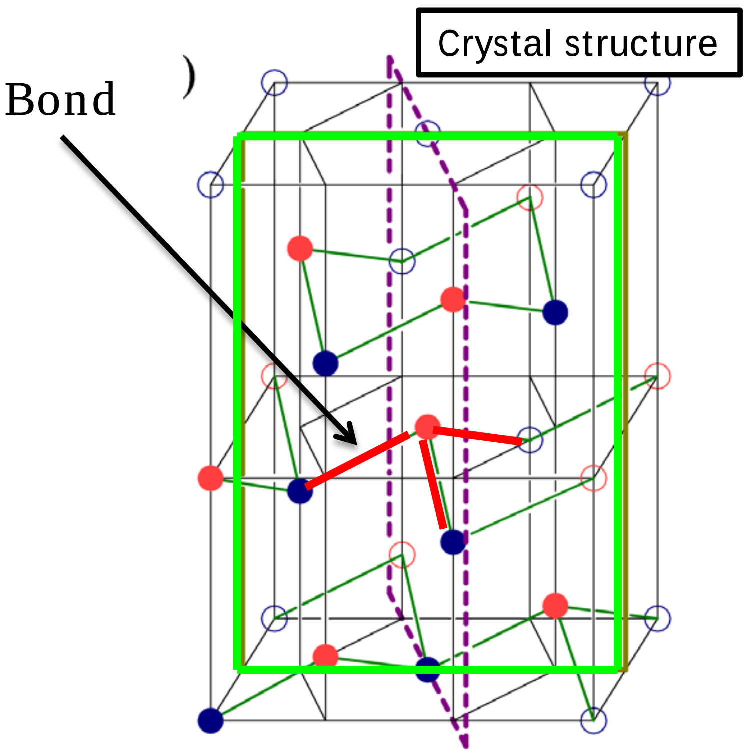

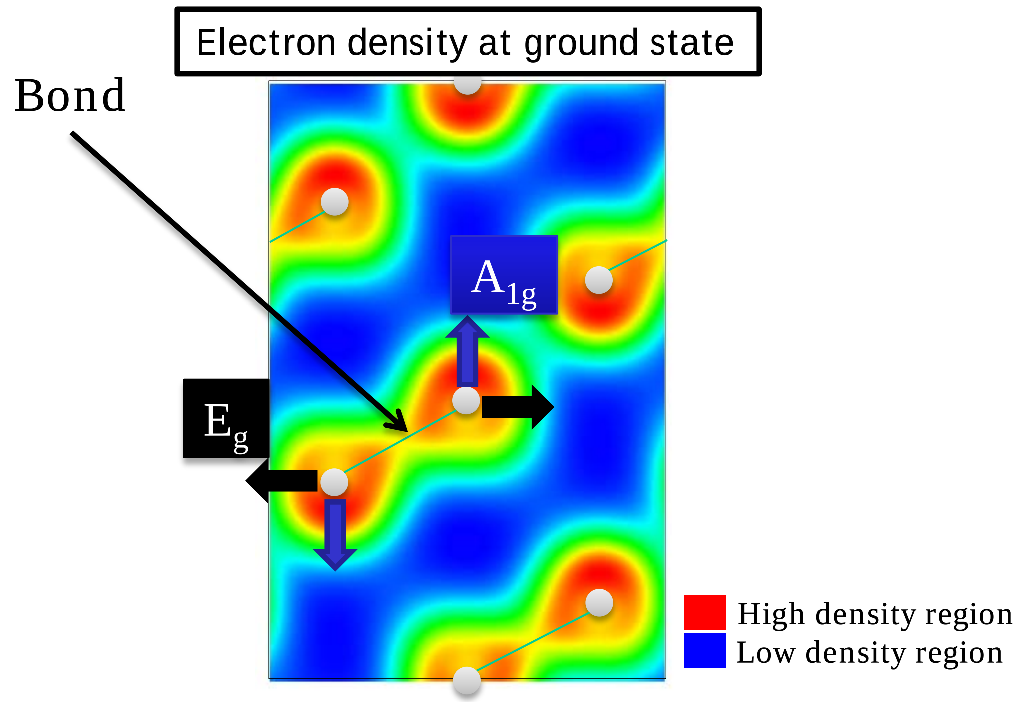

Each atom have three bonds
Only one bond on plane
Other two bonds are out of plane

There are two modes:
A1g and Eg (doubly degenerate)

Electron density under laser pulse

Y. Shinohara et.al, submitted to J. Chem. Phys.

Increasing
Decreasing

Electron density at ground state

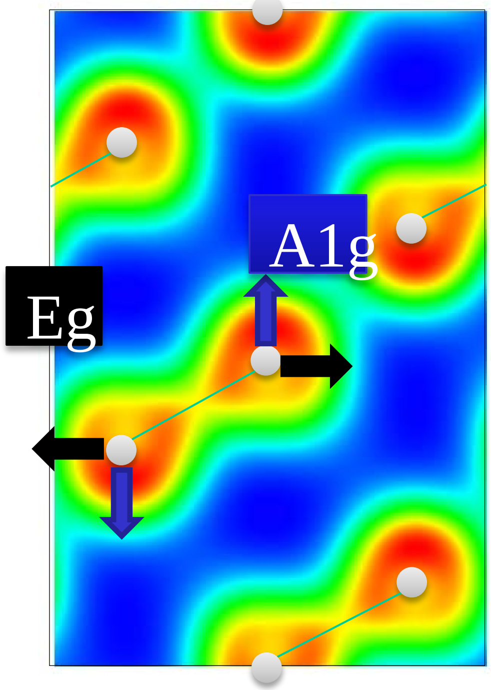

Density difference on plane-1

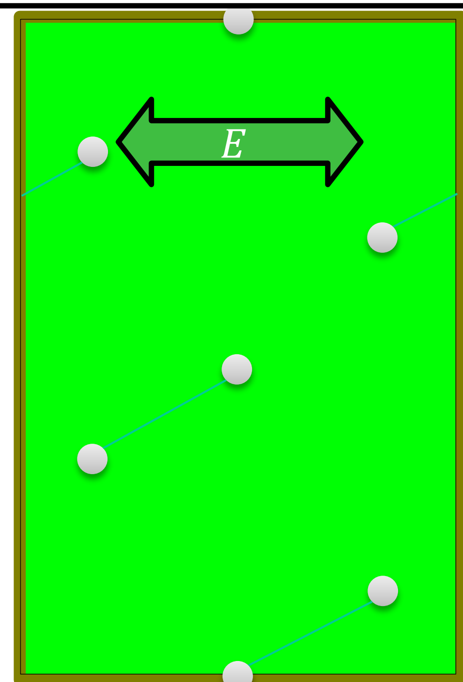

Including electric field

Density difference on plane-2

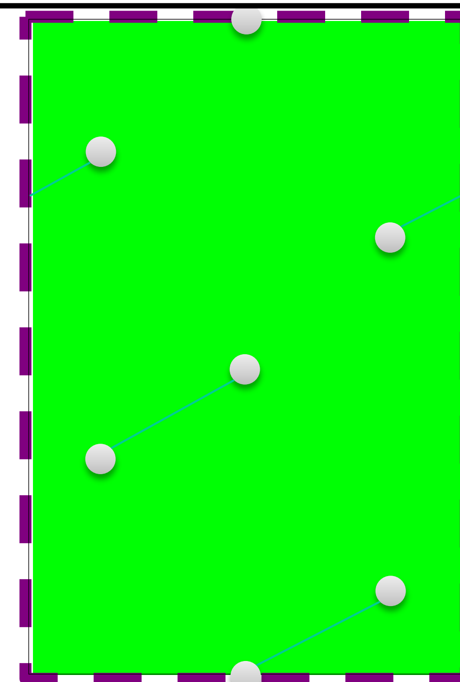

Out of electric field

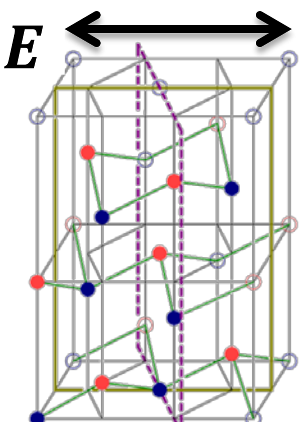

During laser pulse: electrons moves atom to atom
After laser pulse ends: bonding electrons are reduced

Density change and force

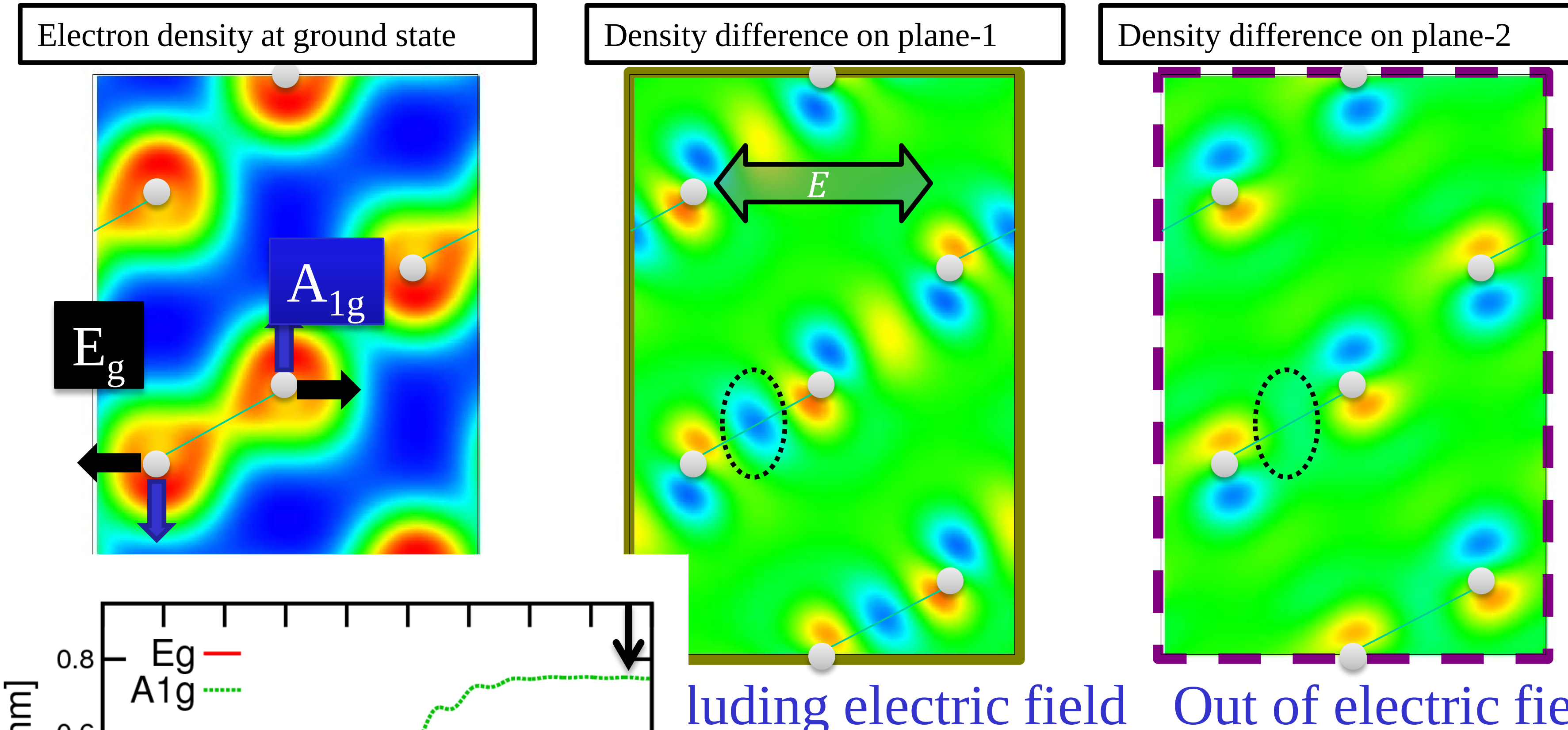

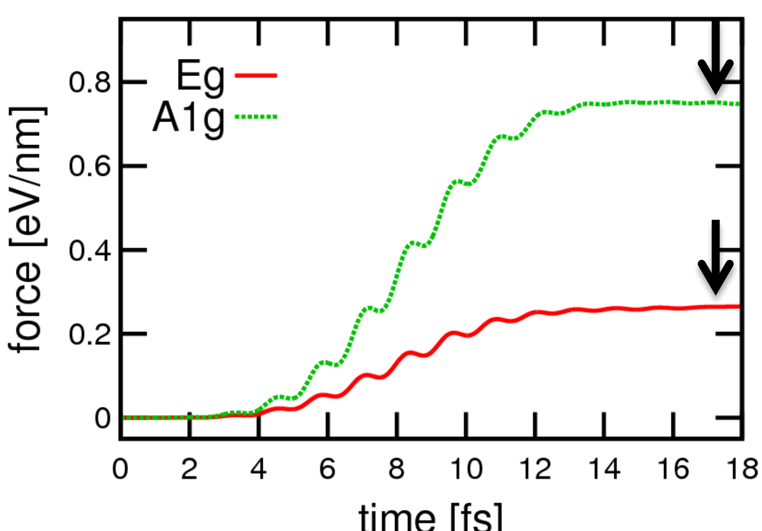

Force is dominated by real-excitation (removal of bonding electrons)

Coherent phonon measurements in Sb

- Most popular material for coherent phonon generation
- Observed two modes: A_{1g}, E_g

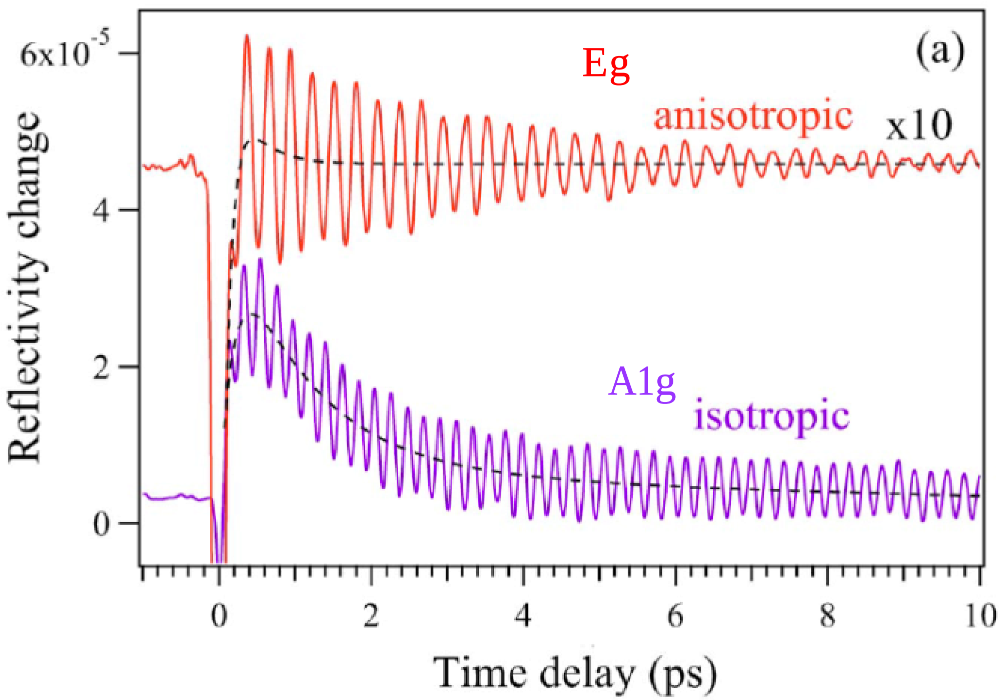

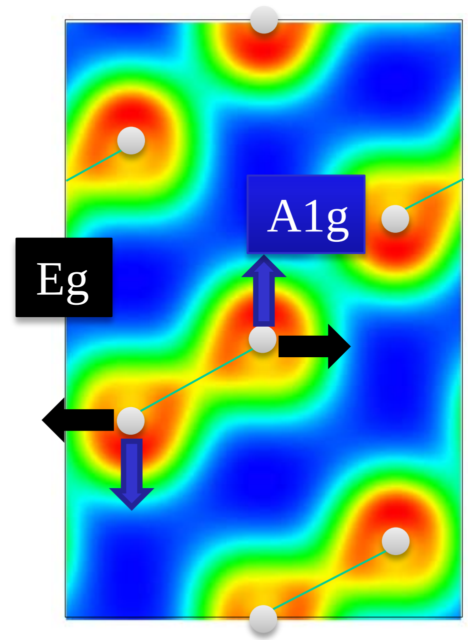

K. Ishioka, M Kitajima, and O. Misochko, J. Appl. Phys. **103**, 123505 (2008)

However, calculation is not consistent with measurement. Experimentally, A_{1g}: displacive, E_g: impulsive.

TDDFT calculation for coherent phonon in Si

Y. Shinohara , et al., Phys. Rev. B. **82**, 155110 (2010)

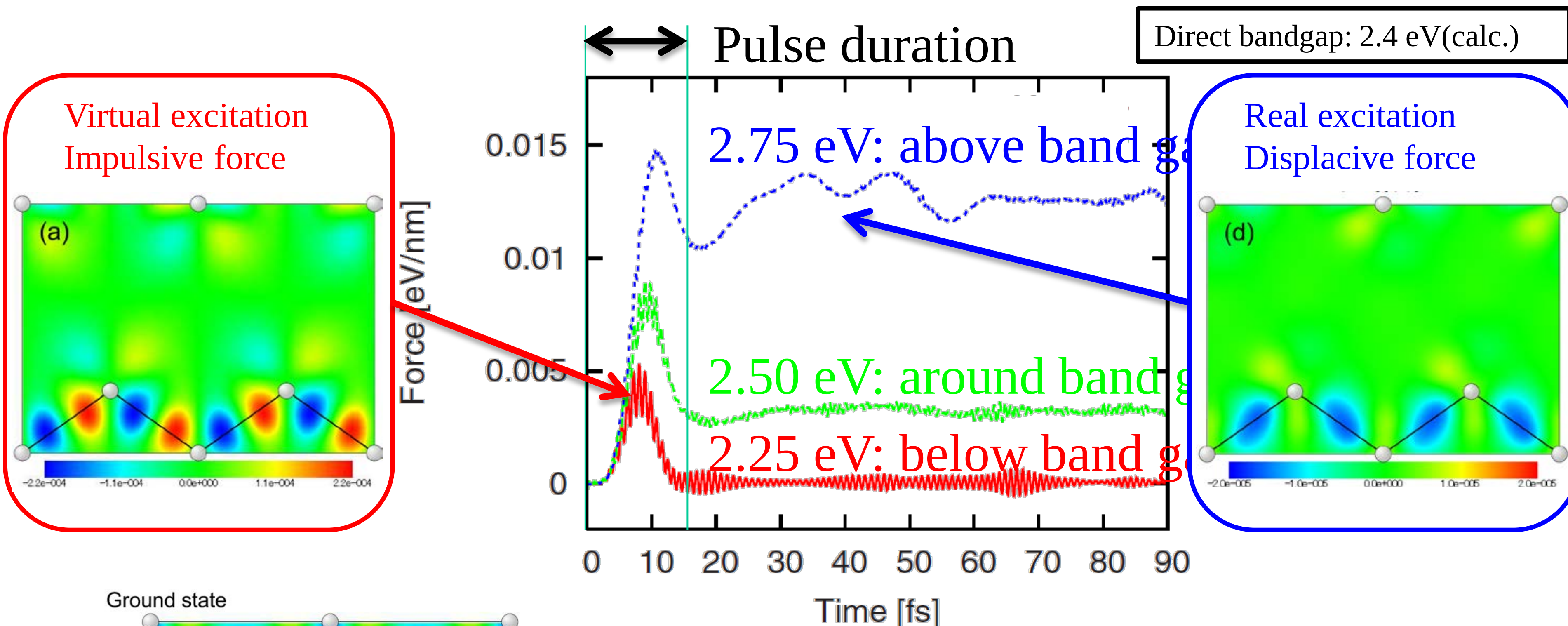

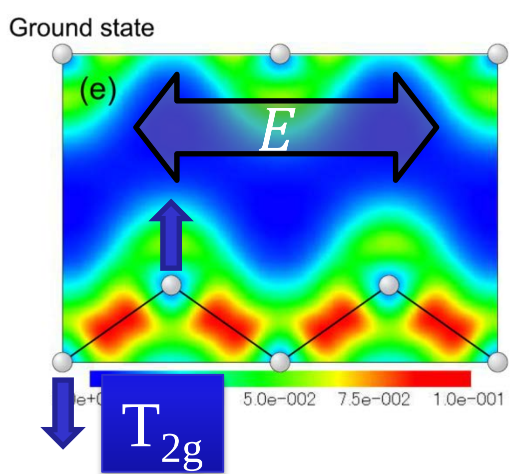

When laser frequency is below the direct gap, impulsive (Raman tensor) force is visible.

CONTENTS

1. A frontier in light - matter interaction : intense and ultrashort
   - Theories and computations required in current optical sciences -

2. Real-time and real-space calculation for electron dynamics in solid
   - time-dependent band calculation, treatment of boundaries. -

3. Electron and phonon dynamics in solid for a given electric field
   - Dielectric function, coherent optical phonon, optical breakdown, … -

4. Coupled Maxwell + TDDFT multiscale simulation
   - First-principles simulation for macroscopic electromagnetic field in intense regime,
     Dense electron-hole plasma induced by intense laser pulses -

Weak field regime: Standard approach for light-matter interaction

Electromagnetism:

Maxwell equation for macroscopic fields,
E, D, B, H

Constitution relation

$$D = D[E] = \varepsilon(\omega)E$$

Quantum Mechanics:

Perturbation theory to calculate linear susceptibilities,
$\varepsilon(\omega)$

Intense laser pulse induced nonlinear electron dynamics

Quantum mechanics is useful to calculate nonlinear susceptibilities as well.

$$D = D[E] = \varepsilon(\omega)E + \chi^{(2)}E^2 + \chi^{(3)}E^3 + \cdots$$

Further increase of laser pulse intensity

Perturbative expansion is no more useful.
Dense electron-hole plasma, Optical breakdown, etc.

$$\Downarrow$$

We need to solve couple Maxwell + Schrodinger dynamics.

We solve coupled Maxwell + Schroedinger equations.

Maxwell equation
describing electromagnetic field

Time-dependent density-functional theory
describing electron dynamics

$$E(\vec{r},t), \quad B(\vec{r},t)$$

$$\psi_i(\vec{r},t)$$

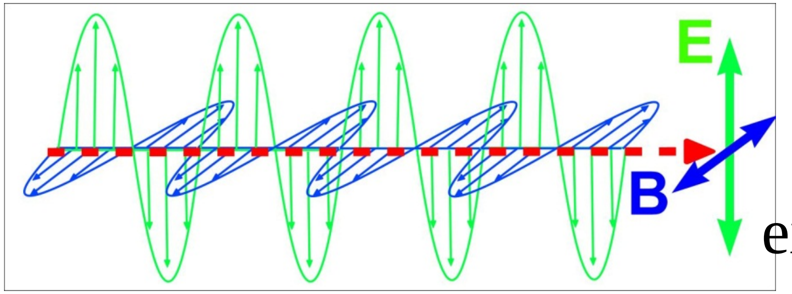

polarization

external field

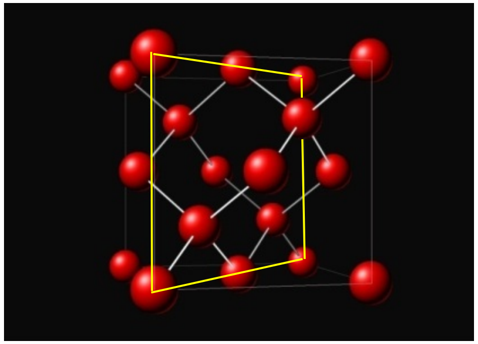

[μm] Different spatial scales [nm]

Time-dependent Kohn-Sham eq.

$$i\hbar\frac{\partial}{\partial t}\psi_i = \frac{1}{2m}\left(-i\hbar\vec{\nabla}+\frac{e}{c}\vec{A}\right)^2\psi_i - e\phi\psi_i + \frac{\delta E_{xc}}{\delta n}\psi_i$$

$$n = \sum_i |\psi_i|^2 \qquad \vec{j} = \frac{1}{2im}\sum_i \psi_i^*\left(-i\hbar\vec{\nabla}+\frac{e}{c}\vec{A}\right)\psi_i - c.c.$$

Maxwell eq.

$$\frac{1}{c^2}\frac{\partial^2\vec{A}}{\partial t^2} - \vec{\nabla}^2\vec{A} = \frac{4\pi}{c}\vec{j} \qquad \vec{\nabla}^2\phi = -4\pi\{en_{ion} - en_e\}$$

Multiscale simulation introducing two spatial grids

Laser pulse irradiation normal on bulk Si

Maxwell eq.

$$\frac{\varepsilon(z)}{c^2}\frac{\partial^2}{\partial t^2}A(z,t)-\frac{\partial^2}{\partial z^2}A(z,t)=0$$

Propagation z-direction, polarization x-direction

$$\vec{A}(\vec{r},t)=A(z,t)\hat{x}$$

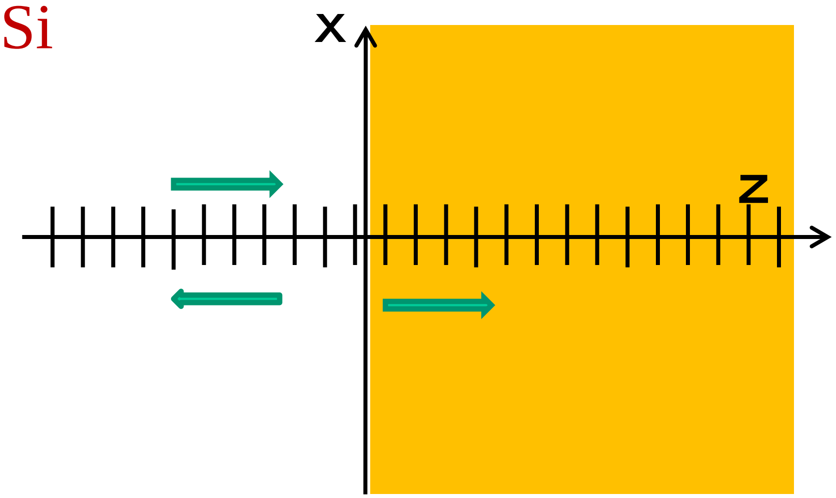

Macroscopic grid

Laser frequency below direct bandgap

$\lambda = 800\text{nm}, \quad \hbar\omega = 1.55\text{eV}$

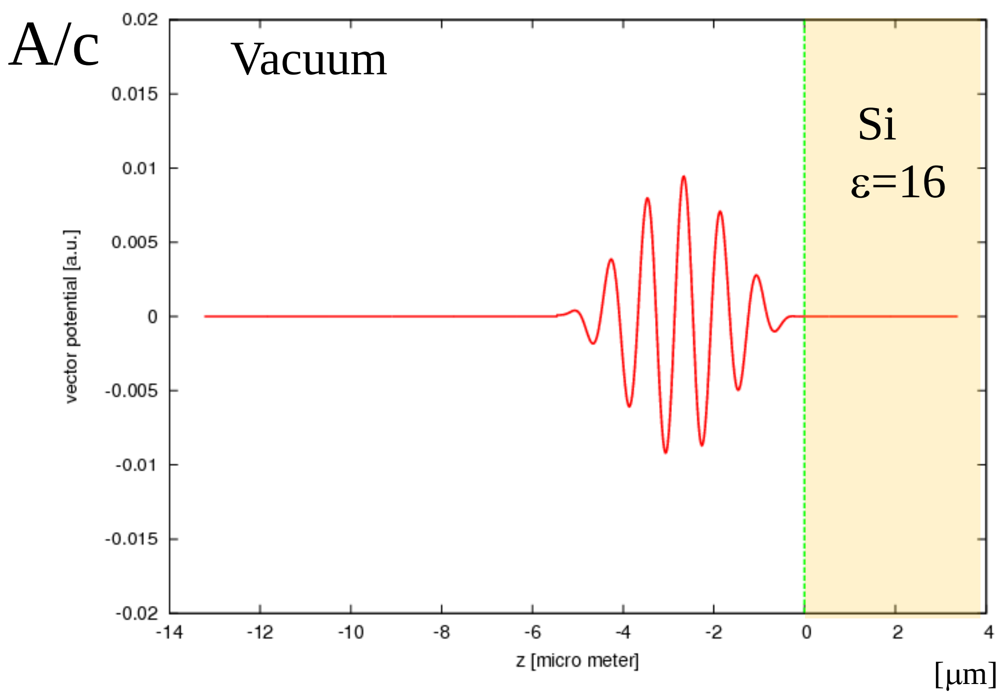

Index of refraction

$$n=\sqrt{\varepsilon}$$

Reflectance

$$R=\left(\frac{1-n}{1+n}\right)^2$$

Velocity of wave

$$v=\frac{c}{n}$$

Multiscale simulation

K. Yabana et.al, Phys. Rev. B85, 045134 (2012).

At each macroscopic grid point,
We consider a unit cell and prepare microscopic grid.

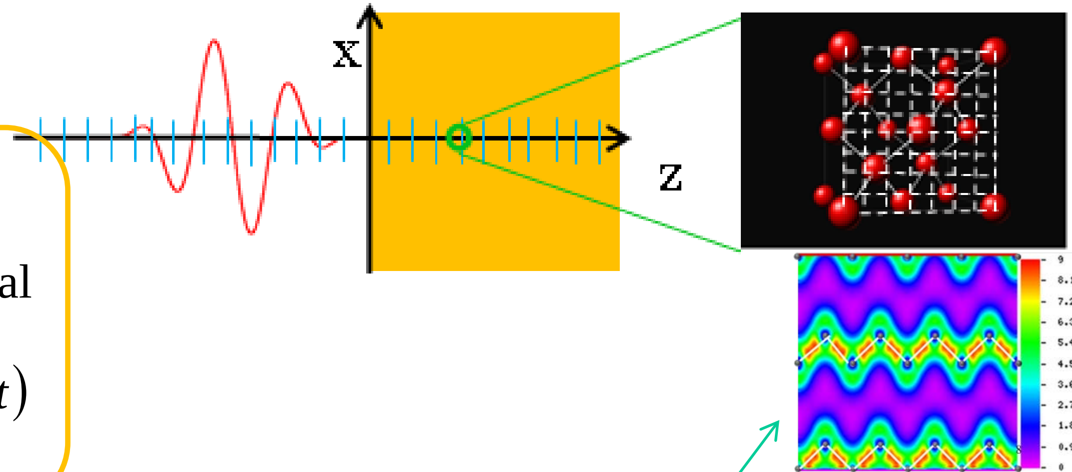

Macroscopic grid points (μm)
to describe macroscopic vector potential

$$\frac{1}{c^2}\frac{\partial^2}{\partial t^2}A(Z,t)-\frac{\partial^2}{\partial Z^2}A(Z,t)=\frac{4\pi}{c}J(Z,t)$$

$J(Z,t)$

Exchange of information by macroscopic current and macroscopic vector potential.

$A(Z,t)$

At each macroscopic points, Kohn-Sham orbitals $\psi_{i,Z}$ are prepared, and described in microscopic grids.

$$i\hbar\frac{\partial}{\partial t}\psi_{i,Z}=\frac{1}{2m}\left(-i\hbar\vec{\nabla}+\frac{e}{c}\vec{A}\right)^2\psi_{i,Z}-e\phi_Z\psi_{i,Z}+\frac{\delta E_{xc}}{\delta n}\psi_{i,Z}$$

$$\vec{\nabla}^2\phi_Z=-4\pi\left\{en_{ion}-en_{e,Z}\right\}$$

$$J(Z,t)=\int_\Omega d\vec{r}\,\vec{j}_{e,Z}$$

$$\vec{j}_{e,Z}=\frac{\hbar}{2mi}\sum_i\left(\psi^*_{i,Z}\vec{\nabla}\psi_{i,Z}-\psi_{i,Z}\vec{\nabla}\psi^*_{i,Z}\right)-\frac{e}{4\pi c}n_{e,Z}\vec{A}$$

Efficient parallelization

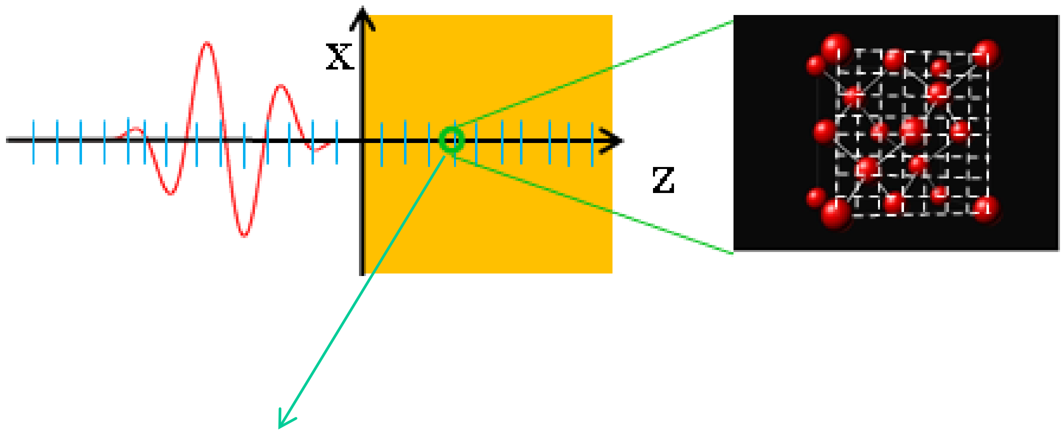

Each CPU calculates electron dynamics at different macroscopic position.

(We also parallelize with repect to k-points)

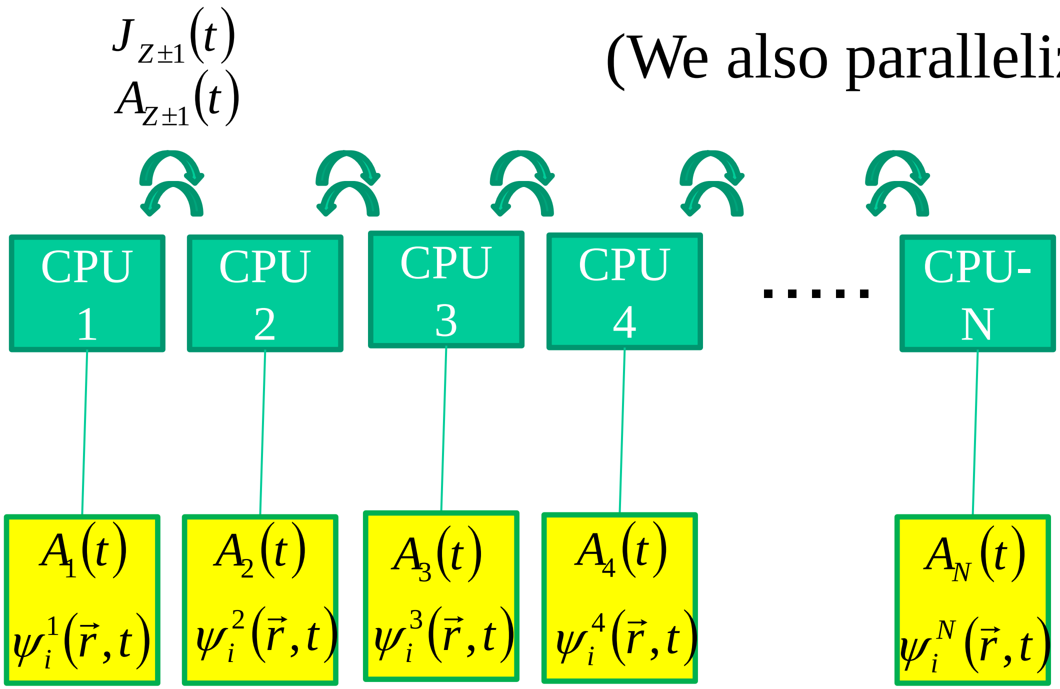

Macroscopic vector potential requires A and j of nearby points to evolve in time.
(only tens of bytes exchanged)

Each CPU calculates nonlinear electron dynamics independently.

Propagation of weak pulse
(Linear response regime, separate dynamics of electrons and E-M wave)

$I=10^{10}$W/cm^2

Laser frequency : 1.55eV :
lower than direct bandgap
2.4eV(LDA)

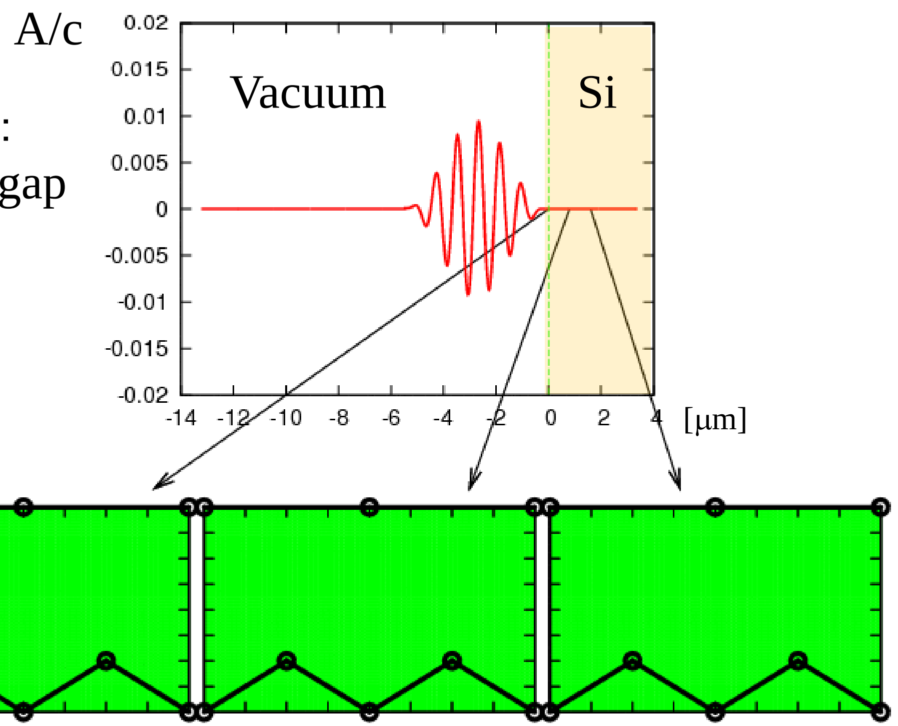

Z=0 [μm]   Z=0.8 [μm]   Z=1.6 [μm]

Propagation of weak pulse
(Linear response regime, separate dynamics of electrons and E-M wave)

I=10^{10}W/cm^2

Laser frequency : 1.55eV :
lower than direct bandgap
2.4eV(LDA)

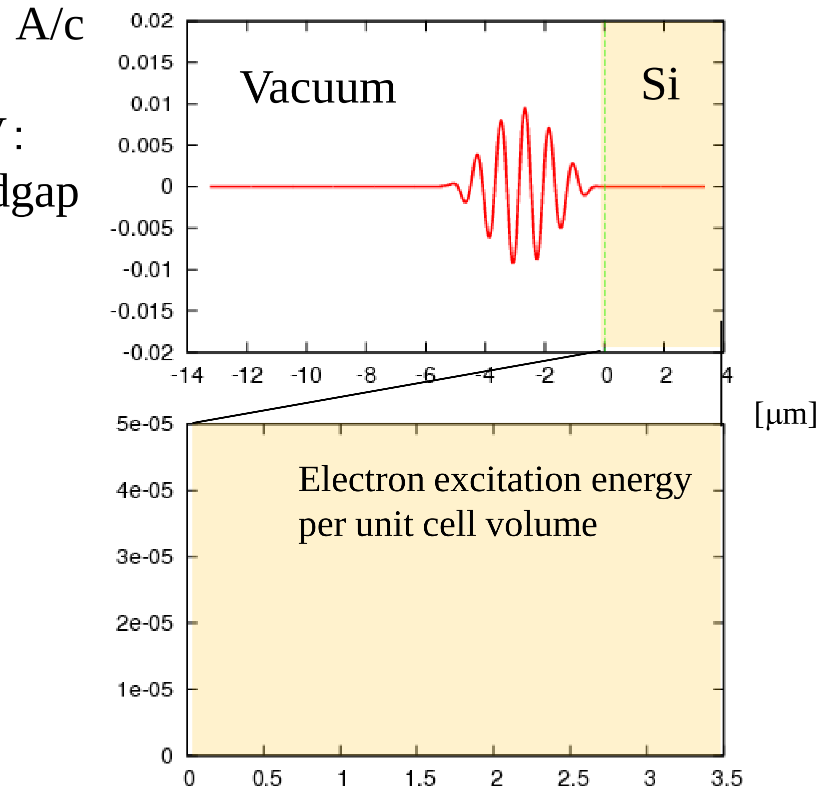

Maxwell+TDDFT vs Maxwell only (constant ε)

Red = Maxwell + TDDFT

Green = Maxwell $\frac{\varepsilon}{c^2}\frac{\partial^2}{\partial t^2}A(z,t)-\frac{\partial^2}{\partial z^2}A(z,t)=0 \qquad \varepsilon=16$

A/c

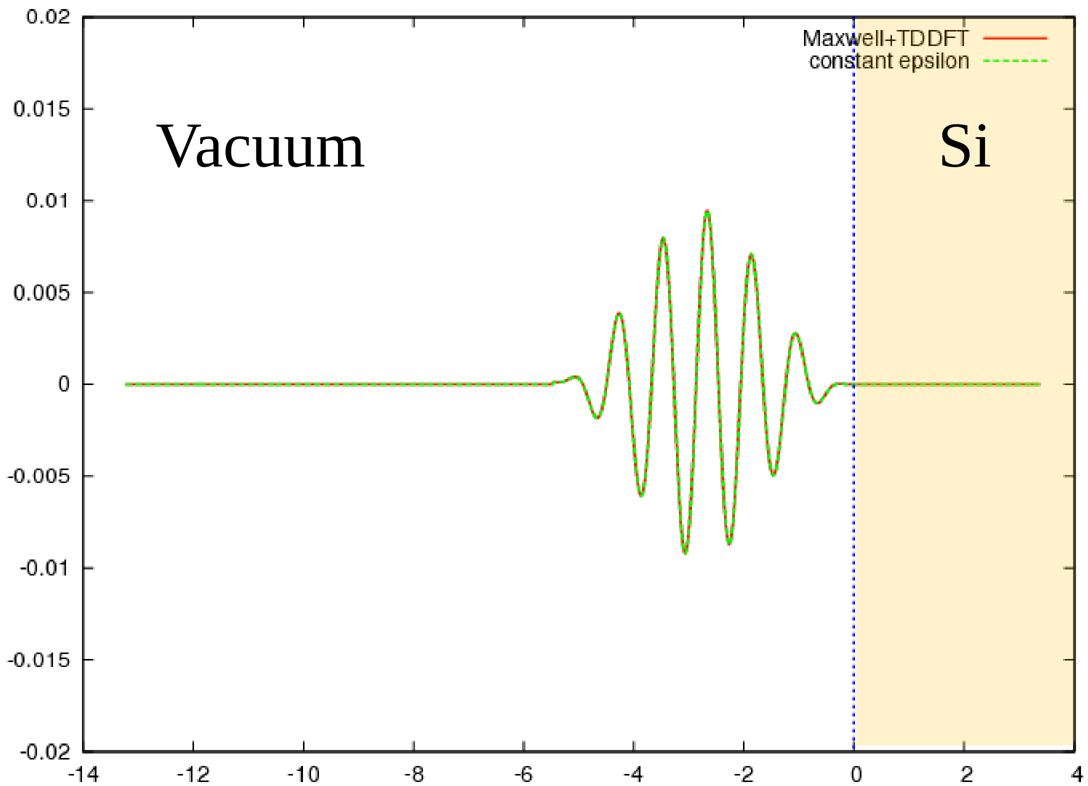

[μm]

In linear regime,
dispersion of dielectric function
Induces

Phase velocity vs group velocity

$$v=\frac{c}{\sqrt{\varepsilon}} \qquad v_g=\frac{c}{\sqrt{\varepsilon}\left(1+\frac{\omega}{2\varepsilon}\frac{d\varepsilon}{d\omega}\right)}$$

Chirp effect is also seen

More intense laser pulse

Maxwell and TDKS equations no more separate.

$I = 5 \times 10^{12} W/cm^2$

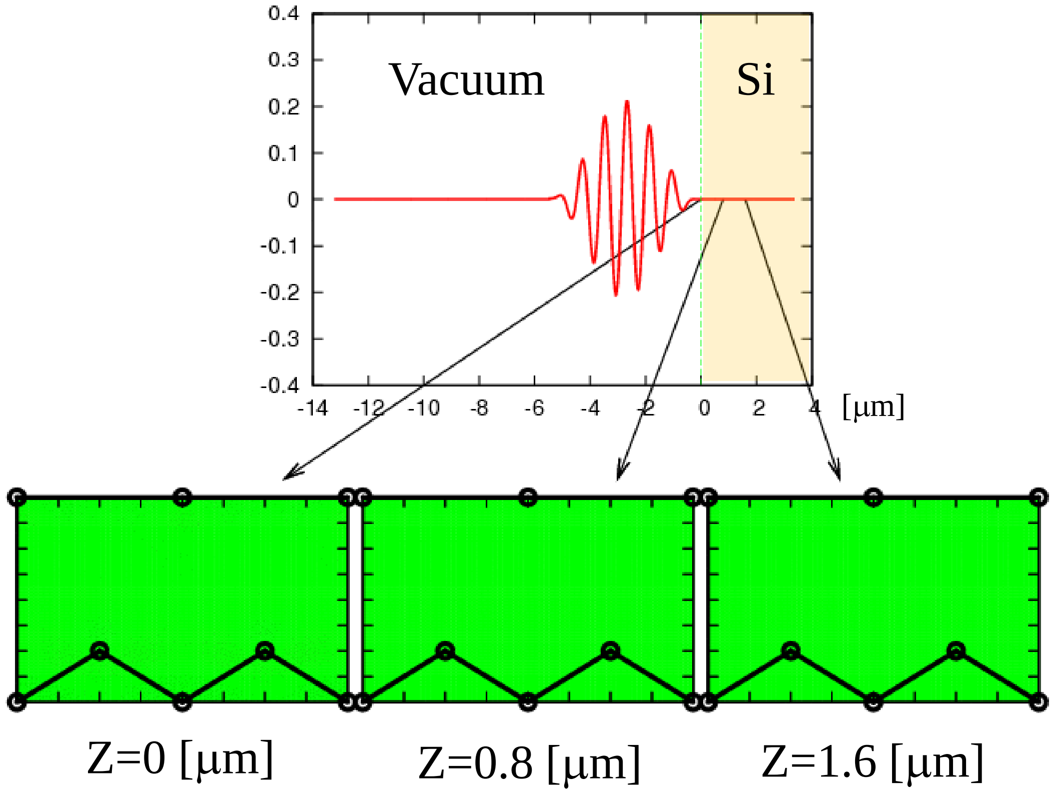

More intense pulse
(2-photon absorption dominates)

$I = 5 \times 10^{12} W/cm^2$

Laser frequency : 1.55eV : lower than direct bandgap 2.4eV(LDA)

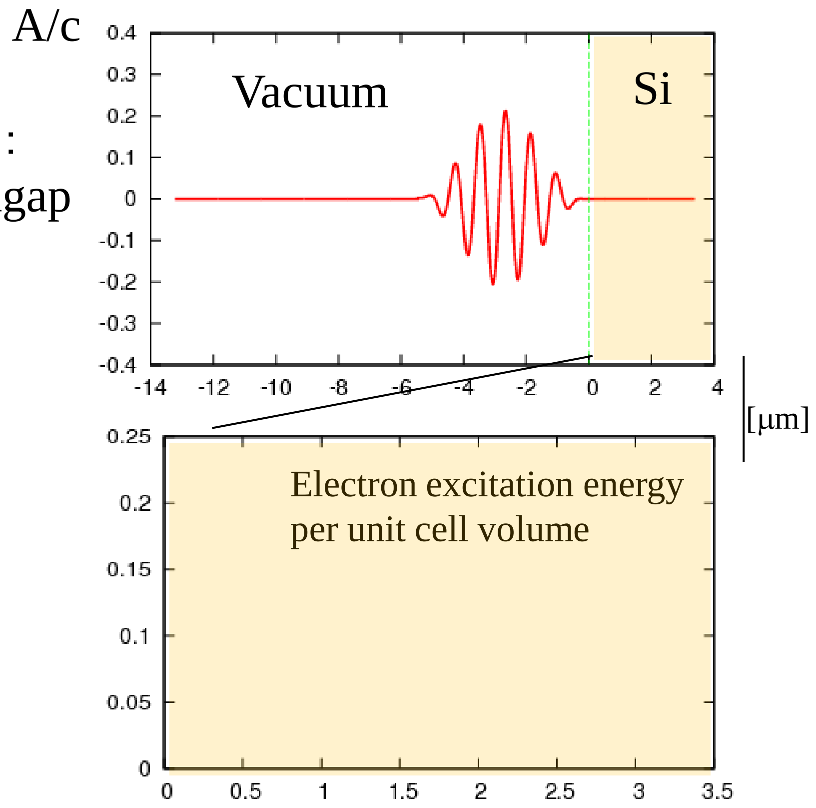

Vector potential and electronic excitation energy
After the laser pulse splits into reflected and transmitted waves

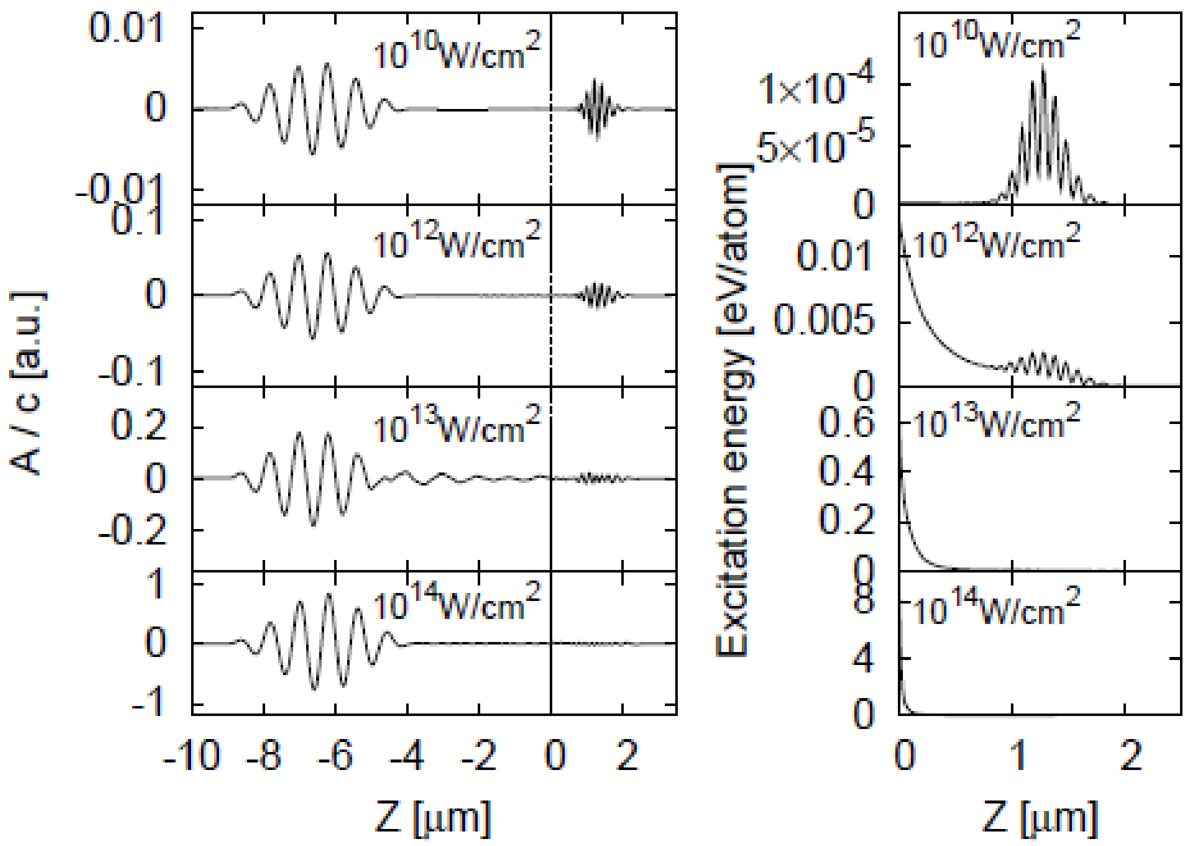

Energy Conservation

Our multiscale equations can be derived from the Lagrangian.

$$L[\psi,\phi,A] = \int dZ \Bigg[\sum_i \int_{\Omega(Z)} d\vec{r}\,\psi^*_{i,Z}(\vec{r},t)\, i\hbar \frac{\partial}{\partial t}\psi_{i,Z}(\vec{r},t)$$

$$-\frac{1}{2m}\left|\left(-i\hbar\vec{\nabla}_r + \frac{e}{c}\vec{A}_Z(t)\right)\psi_{i,Z}(\vec{r},t)\right|^2$$

$$+\int_{\Omega(Z)} d\vec{r}\left\{ e\Big(n_{ion,Z}(\vec{r}) - n_{e,Z}(\vec{r},t)\Big)\phi_Z(\vec{r},t) - E_{xc}[n_Z(\vec{r},t)]\right\}$$

$$+\int_{\Omega(Z)} d\vec{r}\,\frac{1}{8\pi}(\vec{\nabla}_r\phi_Z(\vec{r},t))^2 + \frac{\Omega}{8\pi c^2}\left(\frac{\partial^2\vec{A}_Z(t)}{\partial t^2}\right)^2 + \frac{\Omega}{8\pi}\left(\vec{\nabla}_Z\times\vec{A}_Z(t)\right)^2 \Bigg]$$

We can derive conserved energy which is a sum of

- energy of EM field
- energy of electrons
- interaction energy between them.

$$H = \int dZ \Bigg[\sum_i \int_{\Omega(z)} \frac{1}{2m}\left|\left(-i\hbar\vec{\nabla}_r + \frac{e}{c}\vec{A}_Z(t)\right)\psi_{i,Z}(\vec{r},t)\right|^2$$

$$+\int_{\Omega(Z)} d\vec{r}\left\{\frac{e}{2}(n_{ion} - n_{e,Z}(\vec{r},t))\phi_Z(\vec{r},t) + E_{xc}[n_Z(\vec{r},t)]\right\}$$

$$+\frac{\Omega}{8\pi c^2}\left(\frac{\partial\vec{A}_Z(t)}{\partial t}\right)^2 + \frac{\Omega}{8\pi}\left(\vec{\nabla}_Z\times\vec{A}_Z(t)\right)^2 \Bigg]$$

Energy conservation well satisfied in practical calculations.

Total energy   Energy of EM field   Electron energy

10^{10} W/cm^2	10^{12} W/cm^2	10^{14}W/cm^2
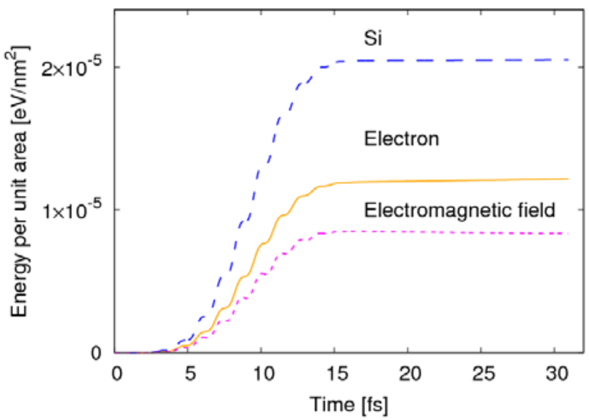	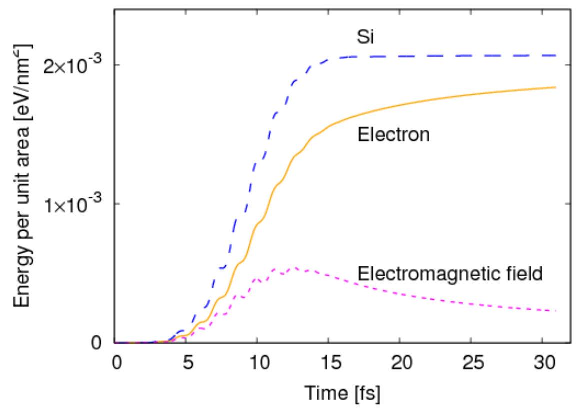	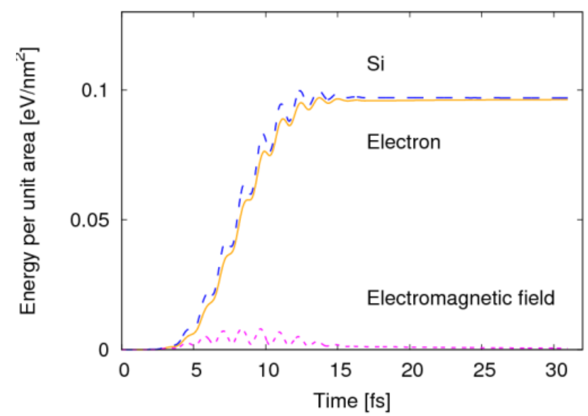

Computational aspect

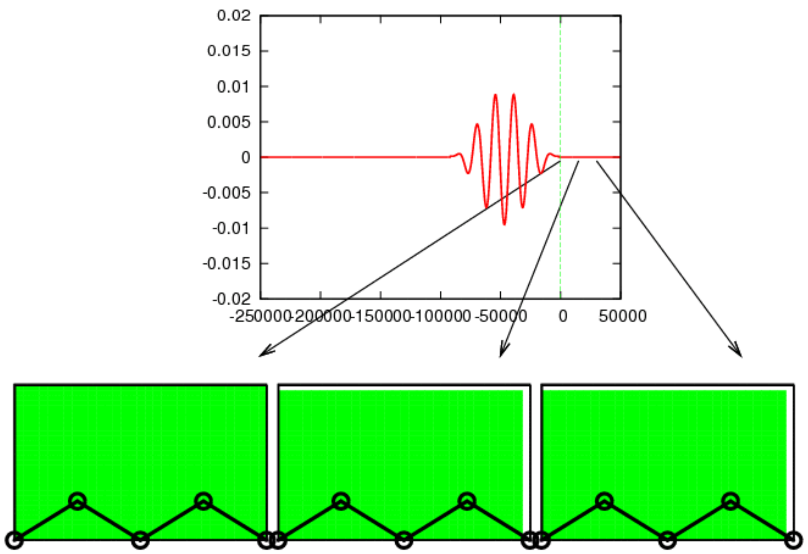

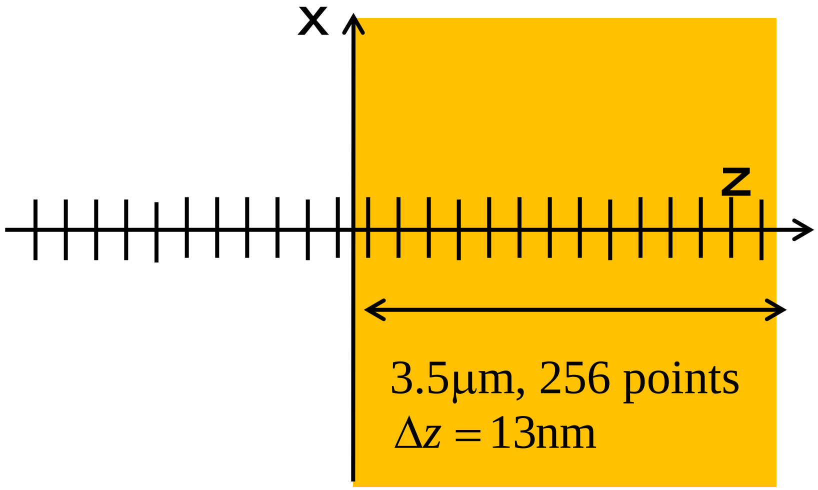

Microscopic (Schroedinger)
spatial grid: 16^3
k-points : 8^3 (reduced by symmetry to 80)
(too small)

Macroscopic (Maxwell)
spatial grid: 256

Time step (commom) = 16,000

Computational costs:

1024 cores (MPI only), 10 hours at SGI Altix ICE 3800EX (ISSP, Univ. Tokyo)

20,480 cores (MPI+openmp), 20 min. at K-Computer

Dense electron-hole plasma generation at the surface modifies dielectric properties at the surface.

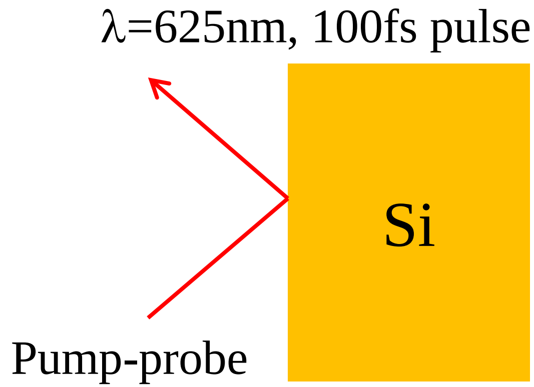

Strong pump-pulse excites electrons at the surface, forming dense electron-hole plasma

K. Sokoowski-Tinten, D. von der Linde, Phys. Rev. B61, 2643 (2000)

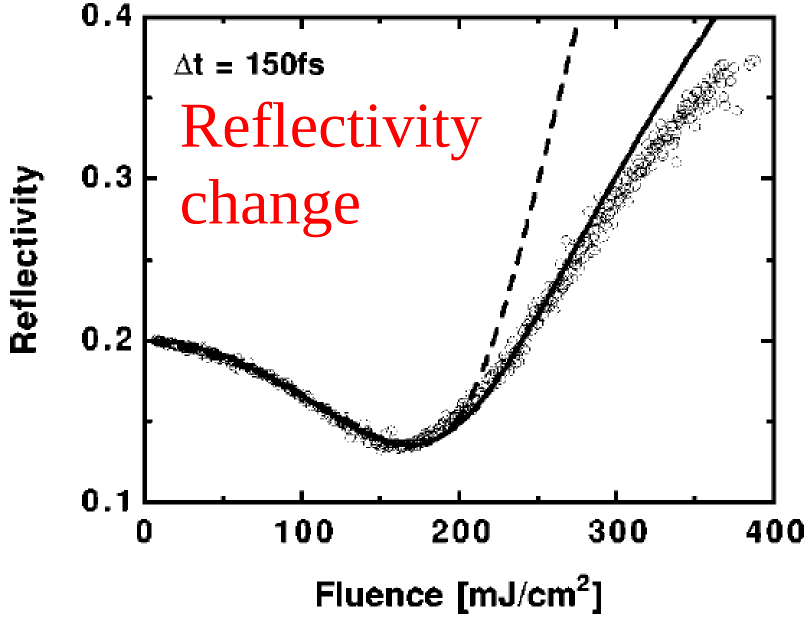

Pump-pulse intensity

Probe-pulse measures change of Dielectric properties.

Drude model fit

$$\varepsilon(n_{ph}) = \varepsilon_{gs} - \frac{4\pi e^2 n_{ph}}{m^*} \frac{1}{\omega\left(\omega + \frac{i}{\tau}\right)}$$

m^*=0.18, τ=1fs

Our Pump-Probe "Numerical Experiment"

I=1x10^{11}W/cm^2,
$h\nu$=1.55eV

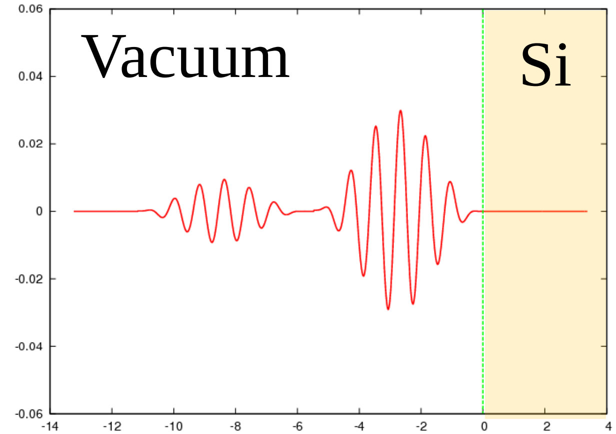

We can calculate

excited electron density at the surface by pump-pulse / reflectivity of probe pulse

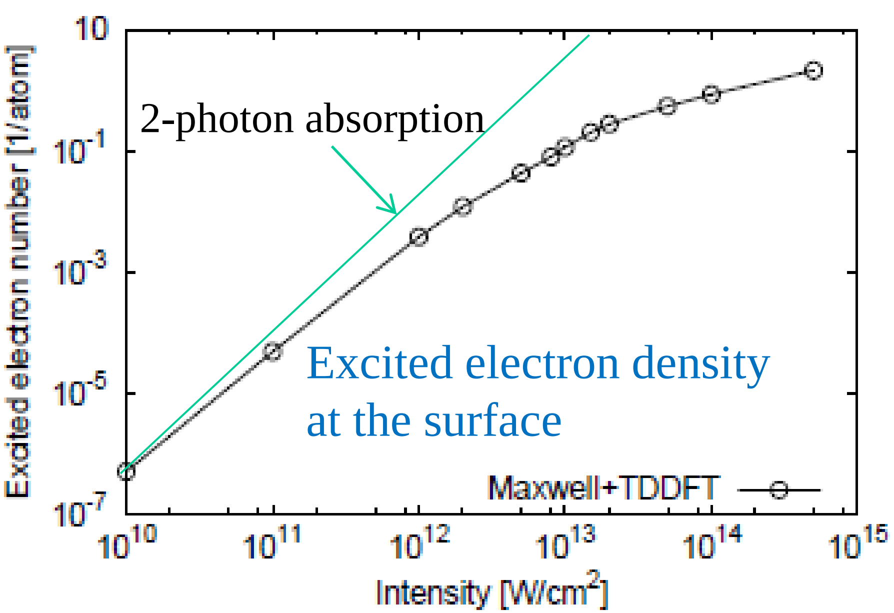

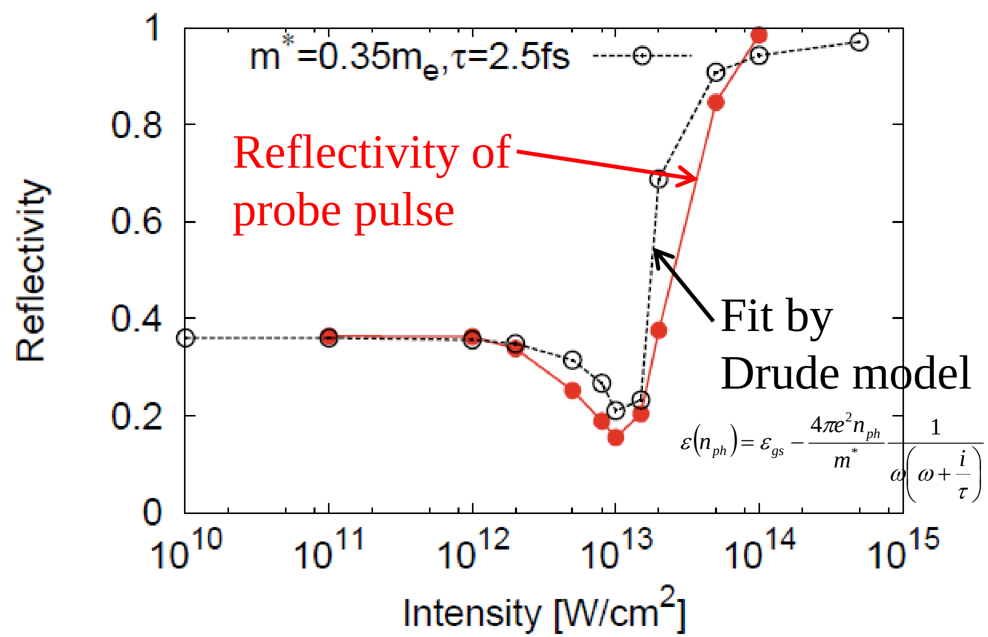

We may extract “dielectric function of excited surface” from numerical pump-probe calculation

$$A(t) = A_i(t) + A_r(t)$$

Decompose vector potential at the surface into incident and reflected components.

$$R(\omega) = \frac{\int dt\, e^{i\omega t} A_r(t)}{\int dt\, e^{i\omega t} A_i(t)}$$

Ratio of two Fourier components gives us a reflectivity as a function of frequency.

$$\Rightarrow \quad R(\omega) = \frac{1 - \sqrt{\varepsilon(\omega)}}{1 + \sqrt{\varepsilon(\omega)}}$$

Dielectric function at the surface when irradiated by 10^{13}W/cm^2 pulse

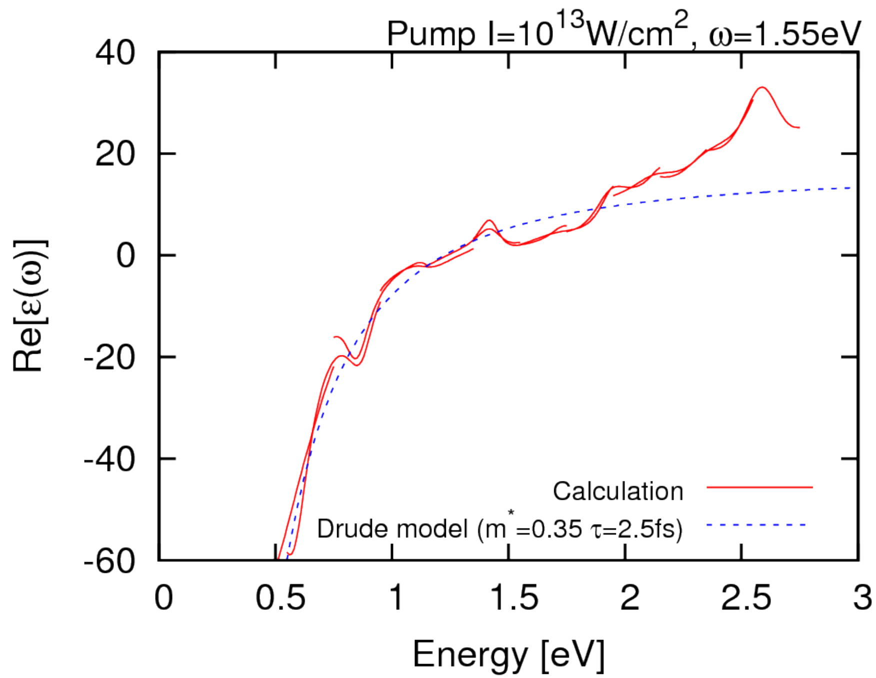

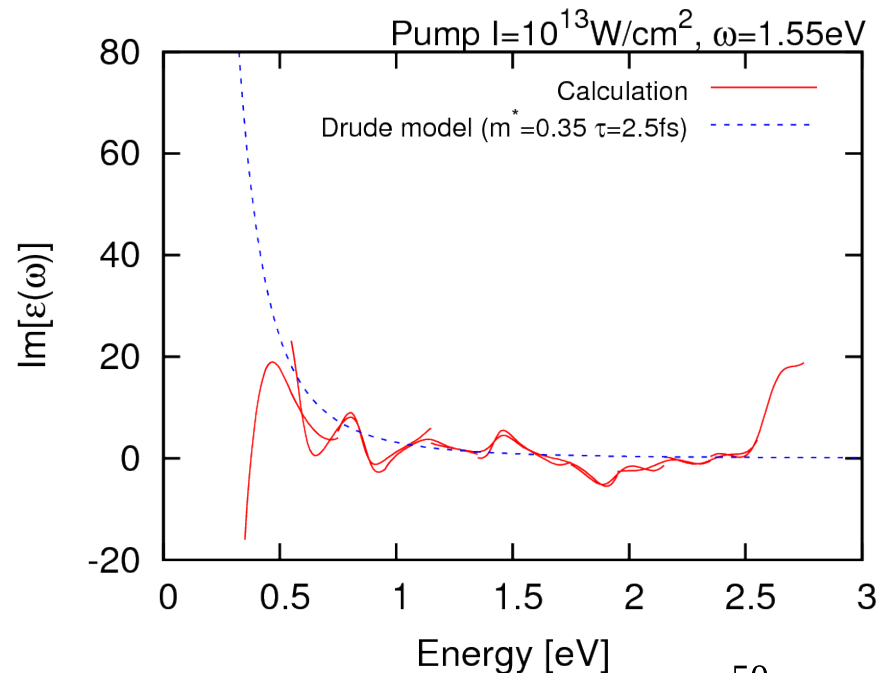

Well described by Drude model (at least for real part).

Change of dielectric function as we increase the pump-pulse intensity.

Increase of electron-hole density enhances metallic response.

$$\varepsilon(n_{ph}) = \varepsilon_{gs} - \frac{4\pi e^2 n_{ph}}{m^*}\frac{1}{\omega\left(\omega + \frac{i}{\tau}\right)}$$

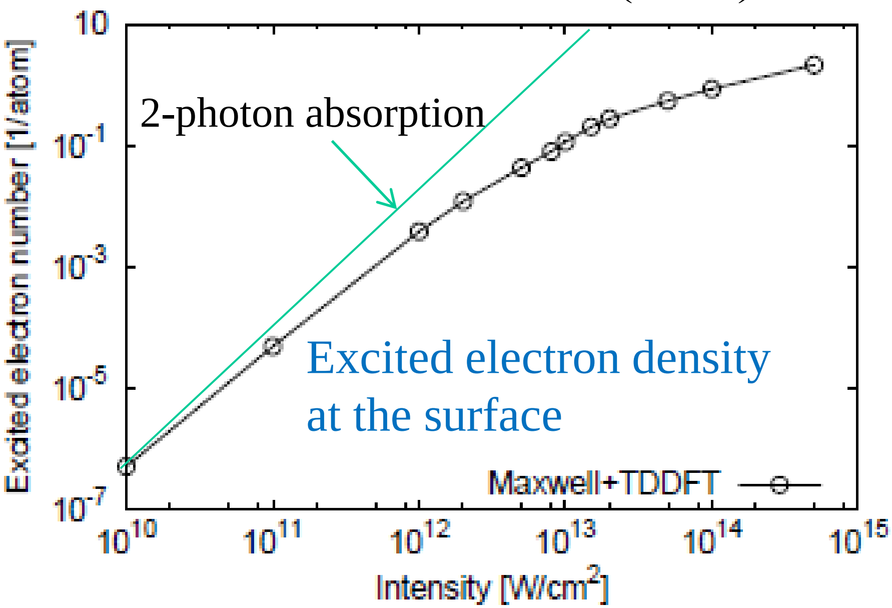

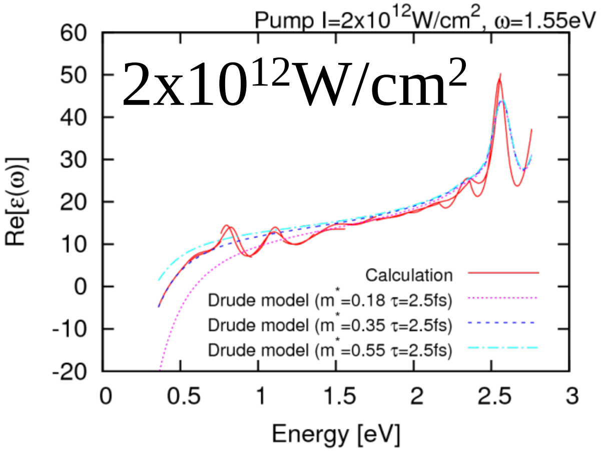

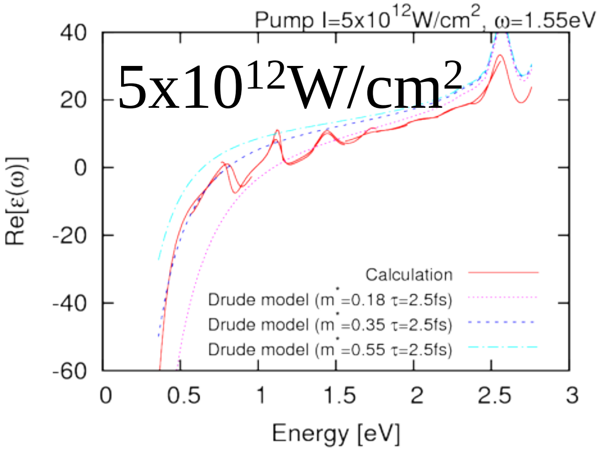

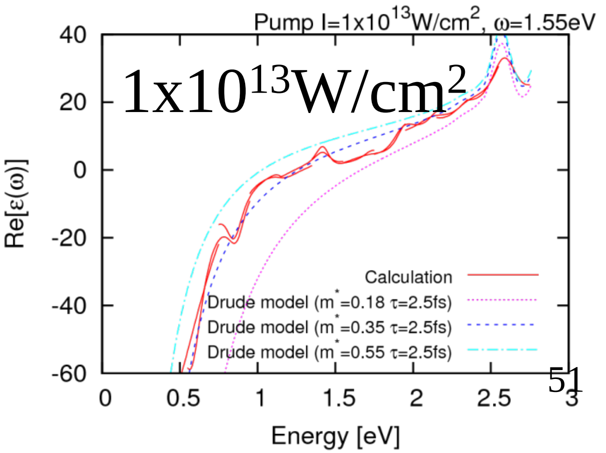

Computational Aspects and Future Prospects

Large computational resources required for multi-scale calculation

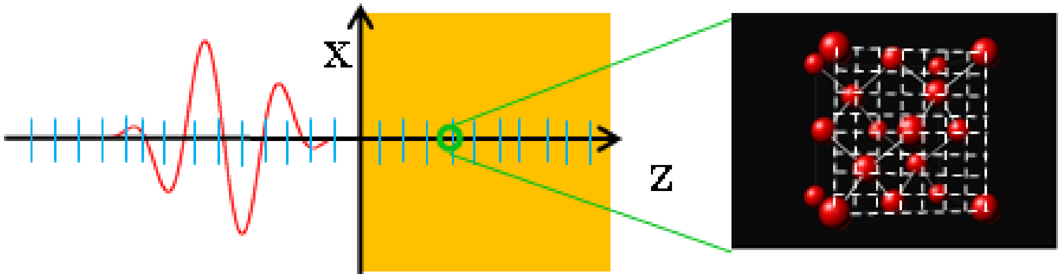

At present

Normal incidence of linearly polarized pulse on Si crystal:

1,000 cores, 10 hours

30,000 cores, 20 min (K-computer, Kobe)

More resources to achieve

- More complex dielectrics (SiO_2, TiO_2, ZrO_2, …) x 10
- Oblique incidence (2-dim) x 50
- Self-focusing (3-dim) x 1000
- Circular polarization (3-dim) x 1000

…

K-Computer, Japan

- 640,000 cores, ¥100,000,000,000

Summary

Electron dynamics in bulk periodic solid by real-time TDDFT

- First-principles description of electron dynamics in femto- and atto-second time scale

- Applications to
    - dielectric function (linear response)
    - coherent phonon generation
    - optical breakdown

Coupled Maxwell + TDDFT multi-scale simulation

- Promising tool to investigate laser-matter interaction

- Requires large computational resources, a computational challenge

- Further developments necessary

  Surface treatment, longitudinal electromagnetic wave, 2D,3D propagation, collision effects (e-e, e-v)